GENETICS, 2022, 221(1), iyac029
https://doi.org/10.1093/genetics/iyac029
Advance Access Publication Date: 15 February 2022
Fungal Genetics and Genomics

A-to-I mRNA editing controls spore death induced by a fungal meiotic drive gene in homologous and heterologous expression systems

Jessica M. Lohmar [1], Nicholas A. Rhoades [2], Tejas N. Patel [2], Robert H. Proctor [1], Thomas M. Hammond [2,*] and Daren W. Brown [1,*]

[1]USDA, Agricultural Research Service, National Center for Agricultural Utilization Research, Mycotoxin Prevention and Applied Microbiology Unit, Peoria, IL 61604, USA,
[2]School of Biological Sciences, Illinois State University, Normal, IL 61790, USA

*Corresponding author: USDA, Agricultural Research Service, National Center for Agricultural Utilization Research, Mycotoxin Prevention and Applied Microbiology Unit, 1815 N. University St., Peoria, IL 61604, USA. Email: daren.brown@usda.gov; *Corresponding author: 346 Science Laboratory Building, School of Biological Sciences, Illinois State University, Normal, IL 61790, USA. Email: tmhammo@ilstu.edu

Abstract

Spore killers are meiotic drive elements that can block the development of sexual spores in fungi. In the maize ear rot and mycotoxin-producing fungus *Fusarium verticillioides*, a spore killer called Sk^K has been mapped to a 102-kb interval of chromosome V. Here, we show that a gene within this interval, *SKC1*, is required for Sk^K-mediated spore killing and meiotic drive. We also demonstrate that *SKC1* is associated with at least 4 transcripts, 2 sense (sense-SKC1a and sense-SKC1b) and 2 antisense (antisense-SKC1a and antisense-SKC1b). Both antisense *SKC1* transcripts lack obvious protein-coding sequences and thus appear to be noncoding RNAs. In contrast, sense-SKC1a is a protein-coding transcript that undergoes A-to-I editing to sense-SKC1b in sexual tissue. Translation of sense-SKC1a produces a 70-amino-acid protein (Skc1a), whereas the translation of sense-SKC1b produces an 84-amino-acid protein (Skc1b). Heterologous expression analysis of *SKC1* transcripts shows that sense-SKC1a also undergoes A-to-I editing to sense-SKC1b during the *Neurospora crassa* sexual cycle. Site-directed mutagenesis studies indicate that Skc1b is responsible for spore killing in *Fusarium verticillioides* and that it induces most meiotic cells to die in *Neurospora crassa*. Finally, we report that *SKC1* homologs are present in over 20 *Fusarium* species. Overall, our results demonstrate that fungal meiotic drive elements like *SKC1* can influence the outcome of meiosis by hijacking a cell's A-to-I editing machinery and that the involvement of A-to-I editing in a fungal meiotic drive system does not preclude its horizontal transfer to a distantly related species.

Keywords: spore killer; *SKC1*; *Fusarium*; *Neurospora*; A-to-I editing; RIP; MSUD; fumonisins; gene drive

Introduction

In the late 1860s, the father of modern genetics, Gregor Mendel, was the first to recognize that the inheritance of an organism's traits was predictable. Today, a key tenant of Mendel's Laws of Inheritance is that a gene (allele) present in only 1 parent of a sexual cross will be inherited by 50% of the resulting progeny. Despite this tenant, some genes are inherited at a much higher frequency, often close to 100%. These "selfish" genes are said to drive through meiosis and are referred to as meiotic drive elements (Zimmering *et al.* 1970).

Several meiotic drive elements have been identified in the Ascomycota, a fungal phylum in which sexual spores, ascospores, are produced in sack-like structures known as asci (Raju 1994; Bravo Nunez *et al.* 2018). In the Ascomycota, known meiotic drive elements are called spore killers because they disrupt ascospore production. While most asci have either 4 or 8 ascospores, a spore killer can reduce the number of viable ascospores by half, with most of the survivors inheriting the spore killer genotype.

Among the Ascomycota, spore killers in species of *Podospora* and *Neurospora* have been examined most extensively. *Podospora anserina* has at least 2 groups of spore killers. One group currently consists of a single member (*het-s*) while the other contains many members (the *Spok* family). The *het-s* allele encodes a prion that interacts with an alternate, nonprion forming allele to cause spore death (Dalstra *et al.* 2003; Saupe 2011). In contrast, *Spok* genes encode a single protein that can both kill spores and provide resistance to killing (Grognet *et al.* 2014; Vogan *et al.* 2019). *Neurospora* spp. has 3 spore killers: *Spore killer-1* (*Sk-1*), *Sk-2*, and *Sk-3* (Turner and Perkins 1979). The *Sk-1* locus consists of a single gene responsible for both killing and resistance (Svedberg *et al.* 2021). The *Sk-2* and *Sk-3* loci contain multiple genes and killing and resistances are conferred by different genes. In the *Sk-2* locus, gene *rfk-1* confers *Sk-2*-mediated spore killing, while gene *rsk* confers resistance to killing (Campbell and Turner 1987; Hammond *et al.* 2012; Harvey *et al.* 2014; Rhoades *et al.* 2019). In the *Sk-3* locus, gene *rsk* confers resistance, but the gene that

Received: September 28, 2021. **Accepted:** February 6, 2022

confers killing has not been identified (Hammond *et al.* 2012; Svedberg *et al.* 2018).

In contrast to *Podospora* and *Neurospora*, understanding of spore killers in other genera of the Ascomycota, such as *Fusarium*, is limited. While meiotic analyses of 3 *Fusarium* species, *Fusarium verticillioides*, *Fusarium subglutinans*, and *Fusarium proliferatum*, have identified the presence of spore killing (Kathariou and Spieth 1982; Sidhu 1984; Raju 1994), little is known about the genetic basis of spore killing in these fungi. All 3 species are of agricultural concern because they cause maize ear rot, which is an economically significant disease under some environmental conditions (White 1999). The fungi are also a food and feed safety concern because they produce mycotoxins. Fumonisin (FB) mycotoxin production by *F. verticillioides* is of particular concern because the toxins frequently contaminate maize kernels and have been associated with cancer, neural tube defects, and stunted growth in human populations for which maize is a dietary staple (Marasas 2001; Munkvold *et al.* 2021). FB toxicity is enhanced by coexposure with aflatoxin, a mycotoxin produced by *Aspergillus* species that also infect maize (Carlson *et al.* 2001; Xue *et al.* 2019). Crops contaminated with mycotoxins cause billion-dollar losses world-wide each year. Although efforts to minimize the impact these toxins have on society have been significant, none have resulted in a control strategy that is effective under all conditions.

Analysis of the spore killer system in *F. verticillioides* indicated isolates have either a spore killer (Sk^K) or spore killer sensitive (Sk^S) genotype. An Sk^K x Sk^S cross yielded asci with 4 ascospores, whereas Sk^K x Sk^K and Sk^S x Sk^S crosses yield asci with 8 ascospores. After initial analyses in the early 1980s, Sk^K was mapped to a 102-kb segment of chromosome V (Xu and Leslie 1996; Pyle *et al.* 2016). Comparison of this segment in Sk^K and Sk^S strains of *F. verticillioides* revealed multiple differences, including the presence of a unique, albeit hypothetical, gene in Sk^K strains and its absence in Sk^S strains. This gene was named *Spore Killer Candidate-1* (*SKC1*) (Pyle *et al.* 2016). The objective of the current study was to further characterize *SKC1* and determine whether it is responsible for Sk^K-mediated spore killing in *F. verticillioides*.

Materials and methods

Fungal strains and general propagation methods

Fusarium verticillioides strains (Table 1) were routinely grown on V8 juice agar (V8A) (Tuite 1969) and Carrot agar (CA) at 22°C in an incubator with continuous fluorescent light (Philips F34T12). CA was prepared as described by Klittich and Leslie (1988) except that we hand-peeled and diced large organically grown carrots for use in the medium. *Neurospora* strains (Table 2) were routinely grown on Vogel's minimal medium (VMM, Vogel 1956) at 32°C in an incubator or at room temperature on a benchtop.

Crossing techniques

Crosses of *F. verticillioides* were performed using previously published protocols with some modifications (Klittich and Leslie 1988; Leslie and Summerell 2006). Crosses were incubated at 22°C with continuous white light provided by 2 fluorescent light bulbs and 12-h intervals of longwave ultraviolet light provided by 1 blacklight bulb (General Electric F40T12BL). Conidia from the female parent of each cross were collected from a V8A culture and placed at the center of a 100-mm Petri plate containing 30.0 ml of CA. After incubation for 1 week, the female parent was fertilized with conidia of the male parent by flooding a V8A culture (100 mm Petri plate) of the male parent with 6.0 ml of 2.5% Tween 60. A 2.0-ml aliquot of the resulting conidial suspension was then added to the 1-week-old CA culture of the female parent and spread over the surface with an L-shaped spreader. The female aerial hyphae and conidia were not removed prior to fertilization, rather they were mixed with the male conidia while spreading. The resulting crossing plate was returned to the incubator and washed at 2-day intervals as reported by Cavinder et al. (2012). That is, an 8.0 ml aliquot of 2.5% Tween 60 was spread over the surface of the plate and the resulting mixture of liquid and disrupted tissue was then poured off. Washes continued until perithecia were observed without magnification on the agar surface.

Unidirectional crosses were performed with *Neurospora crassa* strains on synthetic crossing medium as previously described (Hammond *et al.* 2011; Samarajeewa *et al.* 2014). Crosses were performed at room temperature under ambient lighting.

Perithecial dissections

Fusarium verticillioides perithecia were harvested 3 weeks postfertilization under a dissecting microscope, rolled on 5% water agar to remove excess vegetative tissue, and squashed under a coverslip in 25% glycerol. Perithecial contents (asci) were examined by standard light microscopy. *N. crassa* perithecia were harvested 12–16 days postfertilization (dpf) under a dissecting microscope and placed in a drop of 50% glycerol on a microscope slide. Syringe needles were used to tease perithecial contents into the surrounding liquid and remove vegetative debris and perithecial wall fragments. The perithecial contents were overlayed with a coverslip prior to examination by standard light microscopy.

General molecular techniques

FungiDB was used to download genome information for *F. verticillioides* and *N. crassa* (Basenko *et al.* 2018). Fungal DNA was routinely isolated with the Quick-DNA Fungal/Bacterial Miniprep Kit (Zymo Research, D6005) or with the Mini Genomic DNA Kit for Plants and Fungi (IBI Scientific, IB47231). PCR was typically performed with Primestar Polymerase (Clontech) or Q5 DNA polymerase (New England BioLabs). The sequences of all primers used in this study are provided in Supplementary Table 1. Gel extraction and DNA/PCR-product purification were performed with the PureLink Quick Gel Extraction Kit (Invitrogen, K210012) or the GEL/PCR DNA Fragment Extraction Kit (IBI Scientific, IB47030). Plasmid DNA was typically isolated from *Escherichia coli* using a standard alkaline lysis miniprep protocol. Gel electrophoresis was performed with standard 0.8–2% agarose-TAE (Tris-Acetate-EDTA) gels. Ethidium bromide staining and UV light sources were used to visualize DNA in agarose gels. Routine DNA sequence analysis was performed with Sequencher (Version 5.4.6, Gene Codes Corp.), DNAMAN (Version 7, LynnonBiosoft), MEGA X (Version 10.2.4, Kumar *et al.* 2018), and/or BioEdit (Version 7.2.5, Hall 1999). CLC Genomics Workbench (Version 20.0, Qiagen) and Tablet (Version 1.21.02.08, Milne *et al.* 2010) were used to visualize alignments of reads from genome and RNA sequencing datasets. Sanger sequencing was performed at NCAUR or the University of Illinois Urbana-Champaign CORE sequencing center.

Transformation vector and plasmid construction

Plasmid pJML38.1 contains *SKC1*-flanking sequences on either side of a hygromycin resistance cassette (*HYGB*). The upstream and downstream *SKC1*-flanking sequence were amplified from Fv999 genomic DNA with primer sets 2759/2760 and 2761/2762, respectively. *HYGB* was amplified from plasmid pJML31.1 (Kim *et al.* 2020) with primer set 2763/2764. The *SKC1*-flanking sequences were fused to *HYGB* by PCR with primer set 2767/2768 according to the PCR fusion protocol of Szewczyk *et al.* (2006). The

Table 1. *Fusarium verticillioides* strains.

Name (Aliases)[a]	*SKC1*[b]	*SKC1* RIP[c]	Marker[d]	Mating type	Genetic lineage
Fv149 (FGSC 7600, M-3125)	Absent	No	None	*MAT1-1*	Sk^S
Fv999 (FGSC 7603, M-3120)	Native	No	None	*MAT1-2*	Sk^K
Δ*SKC1*::*HYGB* (tJML33.1)	Replaced with *HYGB*	No	Δ*SKC1*::*HYGB*	*MAT1-2*	Sk^K
Δ*SKC1*::*GENR* (tJML34.46)	Replaced with *GENR*	No	Δ*SKC1*::*GENR*	*MAT1-2*	Sk^K
Addback-A (tJML69.37)	Native + ectopic	No	$GENR^E$	*MAT1-2*	Sk^K
Addback-B (tJML69.143)	Native + ectopic	No	$GENR^E$	*MAT1-2*	Sk^K
Addback-C (tJML69.253)	Native + ectopic	No	$GENR^E$	*MAT1-2*	Sk^K
Offspring-A3 (tJML69.37 P3)	Native	No	None	*MAT1-1*	$Sk^S \times Sk^K$
Offspring-A5 (tJML69.37 P5)	Native	Yes	None[e]	*MAT1-1*	$Sk^S \times Sk^K$
Offspring-A6 (tJML69.37 P6)	Native	No	None	*MAT1-1*	$Sk^S \times Sk^K$
Offspring-B25 (tJML69.37 P25)	Native	Yes	None	*MAT1-1*	$Sk^S \times Sk^K$
Fv-*SKC1*$^{TAG>TAA}$ (tJML56.208)	Native *SKC1*$^{TAG>TAA}$ + ectopic	No	None	*MAT1-2*	Sk^K
Offspring-C11 (tJML56.208 P11)	Native *SKC1*$^{TAG>TAA}$	No	None	*MAT1-2*	$Sk^S \times Sk^K$
Offspring-C37 (tJML56.208 P37)	Native *SKC1*$^{TAG>TAA}$	No	None	*MAT1-2*	$Sk^S \times Sk^K$

[a] Strain sources: Fv149 and Fv999 (Leslie *et al.* 1992). All other *Fusarium* strains in this study were derived from Fv999 and/or Fv149.
[b] The status of *SKC1* in each strain is indicated. Addback strains carry multiple copies of *SKC1*, 1 at the native locations and 1 or more at ectopic locations. Offspring-A3 and -A6 carry a functional version of *SKC1* at the native location. Offspring-A5 and -B25 carry nonfunctional versions of *SKC1* at the native location and at ectopic locations(s).
[c] The presence of multiple copies of *SKC1* in Addback strains correlates with RIP-like mutations in the copy/copies of *SKC1* passed to some descendants (see Table 3).
[d] The status of selectable markers in each strain is indicated. Each addback strain carries at least 1 ectopic copy of $GENR^E$.
[e] Offspring-A5 has multiple, nonfunctional copies of *GENR*, due likely to RIP.

Table 2. *Neurospora crassa* strains.

Name	Short name	Genotype
F2-26 (RTH1005.2)	wt	*rid; fl a*
ISU-3037 (RTH1623.2)	*sad-2*$^{\Delta}$	*rid; fl; sad-2*$^{\Delta}$*::hph*$^{+}$ *a*
ISU-4915 (CNR310.1.2)	*SKC1*	*rid his-3*$^{+}$*::SKC1::nat*$^{+}$*; mus-52*$^{\Delta}$*::bar*$^{+}$ A
ISU-4987 (CNR315.1.1)	*SKC1*$^{TAG>TGG}$	*rid his-3*$^{+}$*::SKC1*$^{TAG>TGG}$*::nat*$^{+}$*; mus-52*$^{\Delta}$*::bar*$^{+}$ A
ISU-4988 (CNR324.3.2)	*SKC1*$^{TAG>TGA}$	*rid his-3*$^{+}$*::SKC1*$^{TAG>TGA}$*::nat*$^{+}$*; mus-52*$^{\Delta}$*::bar*$^{+}$ A
ISU-4989 (CNR325.2.2)	*SKC1*$^{TAG>TAA}$	*rid his-3*$^{+}$*::SKC1*$^{TAG>TAA}$*::nat*$^{+}$*; mus-52*$^{\Delta}$*::bar*$^{+}$ A
P8-43	Host	*rid his-3; mus-52*$^{\Delta}$*::bar*$^{+}$ A

The *Neurospora* strains used in this study are in the Oak Ridge genetic background (Perkins 2004). The *rid* genotype suppresses RIP (Freitag *et al.* 2002). The *his-3* genotype results in histidine auxotrophy, while the *fl* genotype suppresses macroconidiation (Perkins *et al.* 2000). The *mus-52*$^{\Delta}$ allele increases transformation efficiency (Ninomiya *et al.* 2004). The *sad-2*$^{\Delta}$ genotype suppresses MSUD (Shiu *et al.* 2006). Mating types are A and *a*. The *his-3*$^{+}$::SKC1 transgene in strains ISU-4915, ISU-4987, ISU-4988, and ISU-4989 were amplified from genomic DNA with primer set I297/I298 and confirmed to be free of unintended mutations by Sanger sequencing.

amplified fusion product was inserted into the commercial vector pCR-XL-2-TOPO with the TOPO XL-2 Complete PCR Cloning Kit (Invitrogen, K805010) to create pJML38.1.

Plasmid pJML39.1 contains *SKC1*-flanking sequences on either side of a geneticin resistance cassette (*GENR*). The pJML39.1 construction method was nearly identical to the pJML38.1 construction method except that a fragment of DNA containing *GENR* was used in the fusion reaction instead of *HYGB*. *GENR* was amplified from plasmid pGenNotI (Desjardins *et al.* 2004) with primer set 2765/2766.

Plasmid pJML51.2 contains the *SKC1* complementation (i.e. "addback") fragment. pJML51.2 was constructed by amplifying a 2.5-kb product from Fv999 genomic DNA with primer set 2767/2768 and inserting the product into pCR-XL-2-TOPO.

Plasmid pJML53.3 is nearly identical to pJML51.2 except for a single site-directed mutation changing the sense-SKC1a stop codon from TAG to TAA. To construct this plasmid, primer set I1262/I1263 was first used to amplify and insert *SKC1* into pJET1.2 with the CloneJET PCR Cloning Kit (ThermoFisher, K1231) to create plasmid pNR210.1. The G-to-A mutation was generated using the Q5 site-directed mutagenesis kit (New England BioLabs, E0554S) on pNR210.1 with primer set P2080/P2081 to create plasmid pNR229. A 1.3-kb fragment containing *SKC1*$^{TAG>TAA}$ was then amplified from pNR229 with primer set 2915/2916 and fused by PCR to a 997-bp *SKC1* upstream fragment (created with primer set 2759/2914) and a 795-bp *SKC1* downstream fragment (created with primer set 2762/2917) using primer set 2767/2768 to generate a 2.5-kb fragment that was subcloned into pCR-XL-2-TOPO to create plasmid pJML53.3 (*SKC1*$^{TAG>TAA}$).

Plasmid pTH1325.7 contains an *SKC1*-spanning interval of DNA between the *Not*I and *Eco*RI sites of plasmid pNR28.12 (GenBank MH553564.1). The *SKC1* fragment in pTH1325.7 was amplified from Sk^K (Fv999) genomic DNA with primer set I1262/I1263. Plasmids pNR214.4, pNR231.8, and pNR232.1 are nearly identical to pTH1325.7 except for a single site-directed *SKC1* mutation in each plasmid. The Q5 Site-Directed Mutagenesis Kit was used with pNR210.1 (see above) and 3 different primer sets to create the following mutant constructs: *SKC1*$^{TAG>TGG}$ (primer set I2039/I2040), *SKC1*$^{TAG>TAA}$ (primer set I2080/I2081), and *SKC1*$^{TAG>TGA}$ (primer set I2080/I2082). The mutant sequences were then inserted between the *Not*I and *Eco*RI sites of pNR28.12 to create plasmids pNR214.4 (*SKC1*$^{TAG>TGG}$), pNR231.8 (*SKC1*$^{TAG>TAA}$), and pNR232.1 (*SKC1*$^{TAG>TGA}$). All site-directed mutations were verified by Sanger sequencing.

Fusarium and *Neurospora* transformations

The *F. verticillioides* transformation procedure used in this study was modified from previously published protocols (Turgeon *et al.* 1987; Salch and Beremand 1993; Proctor *et al.* 1999) as described below. Conidia were collected from the recipient strain after 7 days of growth on 20 ml of V8A in a 100-mm Petri plate for approximately 1 week into 15 ml of water. The spore suspension

was then filtered through 3 layers of sterile Miracloth (MilliporeSigma, 475855), added to 100 ml of GYP (2% glucose, 0.3% yeast extract, 1% peptone), and incubated at 28°C and 200 rpm until germ tubes were approximately 3–10 times the length of an ungerminated conidium (approximately 8 h).

Germlings were collected by centrifugation at 1,408*g* for 10 min, washed with 10 ml of 0.7 M NaCl, and resuspended in 20 ml of 0.7 M NaCl containing 15 mg/ml Lysing Enzymes (MilliporeSigma, L1412), 40 mg/ml Driselase (MilliporeSigma, D9515), and 0.1 mg/ml chitinase (MilliporeSigma, C6137). The digestion reaction was incubated at 30°C and 100 rpm until most germ tubes had been digested (1–3 h). Protoplasts were collected by centrifugation for 10 min at 1,408*g*, washed once with 10 ml of 0.7 M NaCl, and resuspended in STC buffer (1.2 M sorbitol, 10 mM $CaCl_2$, and 10 mM Tris-HC1, pH 8.0) at a concentration of 5–10 × 10^8 protoplasts/ml.

To replace *SKC1* with *HYGB*, DNA was amplified from pJML38.1 with primer set 2767/2768. To replace *SKC1* with *GENR*, DNA was amplified from pJML39.1 with primer set 2767/2768. To complement Δ*SKC1*::*HYGB* with *SKC1*, 2 DNA molecules were amplified; 1 DNA molecule was amplified from pJML51.2 with primer set 2767/2768, and the other was amplified from pGenNotI with primer set 739/740. For transformation of protoplasts with a single DNA molecule, 15–20 μg of PCR product was added directly to 300 μl of protoplasts. A solution of STC-PCT was freshly prepared by mixing equal volumes double strength (2×) STC with PCT (30% polyethylene glycol 8000, 50 mM $CaCl_2$, and 10 mM Tris-HCl, pH 8.0). A 1.2 ml aliquot of STC-PCT was then added to the transformation reaction (i.e. the DNA + protoplast suspension). After 1-h incubation at room temperature without agitation, 4 ml of STC was added to the transformation reaction, which was followed by the addition of 2 ml of PCT. The transformation reaction was then incubated for 1 h at room temperature without agitation before plating. For cotransformation of protoplasts with 2 DNA molecules, 50–60 μg of each PCR product was added to 600 μl of protoplasts. All other reagent volumes were doubled relative to transformation with one molecule except for the second STC and PCT treatments in which the STC (4 ml) and PCT (2 ml) volumes remained the same.

To plate transformation reactions, the entire reactions were combined with 100 ml of molten (50–55°C) regeneration medium [RGM, 34.2% sucrose, 0.1% yeast extract, 0.1% casein hydrosylate (enzymatic), and 2% agar], poured (in 10-ml aliquots) onto 20 ml of solidified RGM in 100 mm culture plates, and incubated overnight. The next day, the plates were overlaid with 10 ml of molten (50–55°C) 1% water agar containing 600 μg/ml hygromycin B (Thermo Fisher, 10687010) or 1 mg/ml G418 Sulfate (Thermo Fisher, 10131027). After several days, colonies that grew through the water agar layer were transferred to separate 60-mm culture plates containing 10 ml of V8A without antibiotic. After producing conidia, putative transformants were screened by conidial PCR. PCR-positive transformants were single spore purified before additional screening by genome sequencing and/or PCR-based genotyping assays.

Neurospora crassa transformations were performed as described by Rhoades *et al.* (2020). All plasmid-based transformation vectors were linearized by restriction digestion with *SspI* and purified with the GEL/PCR DNA Fragment Extraction Kit. Homokaryotic transformants were obtained by plating dilute concentrations of conidia on selective BDS medium (Brockman and De Serres 1963; Rhoades *et al.* 2020) and screening single-conidium-derived colonies by PCR. Strain CNR310.1.2 was constructed by transforming strain P8-43 with pTH1325.7. CNR315.1.1 was constructed by transforming P8-43 with pNR214.4. CNR324.3.2 was constructed by transforming P8-43 with pNR232.1. CNR325.3.2 was constructed by transforming P8-43 with pNR231.8. The homokaryotic nature of CNR310.1.2, CNR315.1.1, CNR324.3.2, and CNR325.3.2 were confirmed with primer set I297/I298.

Preliminary screening of transformants by conidial PCR

Fusarium verticillioides transformants with the desired genetic modification were screened by conidial PCR essentially as described by Henderson *et al.* (2005). For each transformant, an inoculation loop of conidia (see Henderson *et al.* 2005 for definition) was suspended in 300 μl of TE (10 mM Tris-HCl, 1 mM EDTA, pH 8.0) in a 0.5-ml microcentrifuge tube and heated at 100°C for 10 min in a thermal cycler. After cooling to room temperature, cellular debris was pelleted by centrifuging for 5 min at 9,391*g*. PCR was performed on 2.0 μl of the supernatant with the Phire Plant Direct PCR Master Mix (Thermo Fisher, F170S; 10 μl final reaction volume). The following primer sets were used to screen transformants for (1) Δ*SKC1*::*HYGB*: 2757/2759, 2758/2762, and 2356/2357; (2) Δ*SKC1*::*GENR*: 2695/2759, 2696/2762, and 2356/2357; and (3) *SKC1* and $SKC1^{TAG>TAA}$ addback strains: 2705/2759, 2706/2762, and 2356/2357.

Genome sequencing and analysis

Genomic DNA for sequencing was isolated with the Quick-DNA Fungal/Bacterial Miniprep Kit. DNA libraries were prepared with the Nextera XT DNA Library Preparation Kit for Illumina Systems (FC-131-1096) and 1 ng of genomic DNA. DNA libraries were sequenced with MiSeq Reagent Kit Version 3 and a MiSeq sequencer (Illumina). Raw reads were processed by removing adapters and low-quality reads were trimmed and filtered with CLC Genomics Workbench as previously reported (Brown *et al.* 2020).

RNA isolation

Fusarium verticillioides total RNA was isolated from Sk^K-vegetative tissue, Sk^S-vegetative tissue, and Sk^S × Sk^K perithecia. Vegetative tissues were collected from liquid shaking cultures of Sk^K (Fv999) or Sk^S (Fv149) (100 ml GYP, 200 rpm, 28°C, and ambient light in 500 ml flask), while perithecia were collected from an Sk^S (Fv149) × Sk^K (Fv999) cross, where Sk^S served as female, 20 dpf. The vegetative and perithecial tissue were lyophilized and stored at −80°C or on dry ice until RNA isolation, which was performed as described by Rhoades *et al.* (2019) with the exception that dried rather than fresh perithecia were ground in TRIzol reagent (ThermoFisher, 15596026). The procedure of Rhoades *et al.* (2019) was also used to isolate total RNA from fresh 10 dpf perithecia of an *N. crassa sad-2*$^{\Delta}$ (ISU-3037) × *SKC1* (ISU-4915) cross, where *sad-2*$^{\Delta}$ served as the female parent.

RNA sequencing and analysis

Two strand-specific RNA sequencing datasets were produced in this study. The mycelial dataset was made with a 4-day vegetative culture of Fv999 (described above), while the perithecial dataset was made with 20 dpf perithecia from an Sk^S (Fv149) × Sk^K (Fv999) cross (described above). RNA sequencing was performed on mRNA-enriched total RNA by Novogene (Sacramento, CA, USA). The mRNA enrichment was performed with an oligo(dT)-based method, and sequencing was performed with a PE150-sequencing strategy and Illumina's NovaSeq 6000 sequencing system. Raw reads were filtered by Novogene to remove reads containing adapters, reads containing more than 10%

Table 3. An analysis of *SKC1* mutations in offspring from parents with multiple copies of *SKC1*.

	SKC1 and flanking DNA				*SKC1* coding sequence only			
	Pos: 97,592–98,261				Pos: 97,921–98,223			
	C>T	G>A	other	Total	C>T	G>A	Other	Total
Addback-A (parent)	0	0	0	0	0	0	0	0
Offspring-A3	0	0	0	0	0	0	0	0
Offspring-A5	32	18	0	50	15	13	0	28
Offspring-A6	0	0	0	0	0	0	0	0
Addback-B (parent)	0	0	0	0	0	0	0	0
Offspring-B25	0	15	0	15	0	10	0	10

Mutations are classified as C to T, G to A, and all others (e.g. A to C, A to G). Genome sequencing reads from each strain were mapped to positions 95,939–100,297 of GenBank KU963213.1. This region is present in Sk^K (Fv999) but not Sk^S (Fv149). Mapped reads were examined for mutations. Only mutations present in at least 20% of reads covering each position were counted.

undetermined base sequences, and reads with more than 50% low quality (Phred) base calls. Filtered reads were trimmed in CLC Genomics Workbench using the NGS Core Tools Trim sequences tool set at default values. The Adapter trim list consisted of the 2 Illumina stranded RNA adapter sequences. The Quality trim parameter limit was 0.05 and the Ambiguous trim parameter was set at 2 residues.

To examine *SKC1* transcription, "Read 2" from each pair of reads was mapped to positions 95,939–100,297 of GenBank KU963213.1, which contains *SKC1*, the intergenic sequences flanking *SKC1*, and the predicted coding sequences of *SKC1*'s flanking genes. A custom python script was used to calculate coverage levels and Microsoft Excel was used to produce coverage level charts. Reads that mapped to the reference with more than 2 mismatches were ignored. Coverage levels in the mycelial and perithecial datasets were used to predict transcript boundaries. Specifically, positions with a coverage level greater than 0.5% that of the highest level along the predicted sense or antisense transcripts were included in the transcript models.

RT-PCR and cDNA analysis

For RT-PCR analysis of sense *SKC1* transcripts, first-strand cDNA synthesis was performed on total RNA with the ProtoScript II First Strand cDNA Synthesis Kit (New England BioLabs, E6560S) with the included Randomized Primer Mix. The reverse transcription products were used as templates in PCR reactions with primer set I2070/I2071. RT-PCR products were analyzed by gel electrophoresis, purified by gel extraction, and analyzed by Sanger sequencing with primer I2074. A similar process was used for RT-PCR analysis of antisense *SKC1* transcription except that the reverse transcription step was primed with an antisense *SKC1* specific primer (I2221 or I2222) instead of random primers. The reverse transcription products were used as templates in PCR reactions with primer set I2225/I2226. The resulting PCR products were gel purified, cloned into pJET1.2 (thereby creating plasmids pNR283.1 and pNR283.6), and sequenced by Sanger sequencing.

SCK1 phylogenetic analysis

SKC1 homologs from *Fusarium* species other than *F. verticillioides* were detected by BLASTN analysis of a previously described genome sequence database housed locally in CLC Genomics Workbench (Kim *et al.* 2020; Geiser *et al.* 2021). The sequences were generated locally or downloaded from GenBank/NCBI as previously described (Kim *et al.* 2020; Geiser *et al.* 2021). Query sequence for BLASTN analysis (default parameters of word size of 11, match 2, mismatch -3 with gap costs of existence 5 and extension 2) was the *SKC1* homolog from *F. verticillioides* Fv999. The sequences of the BLASTN hits were retrieved and subjected to phylogenetic analyses as implemented in MEGA X (Kumar *et al.* 2018). First, the homologous *SKC1* ORFs were predicted based on comparison to *SKC1* from *F. verticillioides*. Next, the coding sequences were converted to amino acid sequence, aligned using the MUSCLE method (Edgar 2004), converted back to the nucleotide sequence, and subjected to maximum parsimony (MP) and maximum likelihood (ML) analyses with 500 bootstrap replicates.

Results

Deleting *SKC1* abolishes Sk^K-mediated spore killing

Crosses between Sk^S and Sk^K strains of *F. verticillioides* produce asci with 4 ascospores instead of 8 because of spore killing (Kathariou and Spieth 1982; Raju 1994). To determine if *SKC1* is required for spore killing, we deleted the gene in an Sk^K strain by replacing it with either of the selectable marker genes *HYGB* or *GENR* (Fig. 1a and Supplementary Figs. 1 and 2). When the *SKC1* deletion mutants (*skc1* mutants) were crossed with an Sk^S strain, the resulting asci had 8 ascospores (Fig. 1, c and d). In contrast, asci from control, $Sk^S \times Sk^K$, crosses had 4 ascospores (Fig. 1b). These results indicate that *SKC1* is required for Sk^K-mediated spore killing.

Complementation with *SKC1* restores Sk^K-mediated spore killing

To confirm that *SKC1* is required for spore killing, we cotransformed an *skc1* mutant (Δ*SKC1*::*HYGB*) with 2 DNA molecules: *GENR* and a 3-kb DNA fragment from the wild-type Sk^K locus that included *SKC1*. Our goal was to restore *SKC1* to the Sk^K locus of the *skc1* mutant via homologous recombination by replacing *HYGB* with a wild-type copy of *SKC1* and at the same time introduce *GENR* at an ectopic location (Fig. 2a). Following the cotransformation protocol, we recovered 3 *skc1* mutant-derived transformants with a wild-type copy of *SKC1* reintegrated into the Sk^K locus replacing *HYGB*. The 3 transformants were designated as *SKC1* addback strains Addback-A, Addback-B, and Addback-C (Supplementary Fig. 3). In crosses with an Sk^S mating partner, Addback-A and Addback-B produced some asci with 4 ascospores and some asci with 8 ascospores (Fig. 2, b and c). In contrast, nearly all asci produced from crosses of Sk^S and Addback-C had 4 ascospores (Fig. 2d). Taken together, these results demonstrate that loss of Sk^K-mediated spore killing,

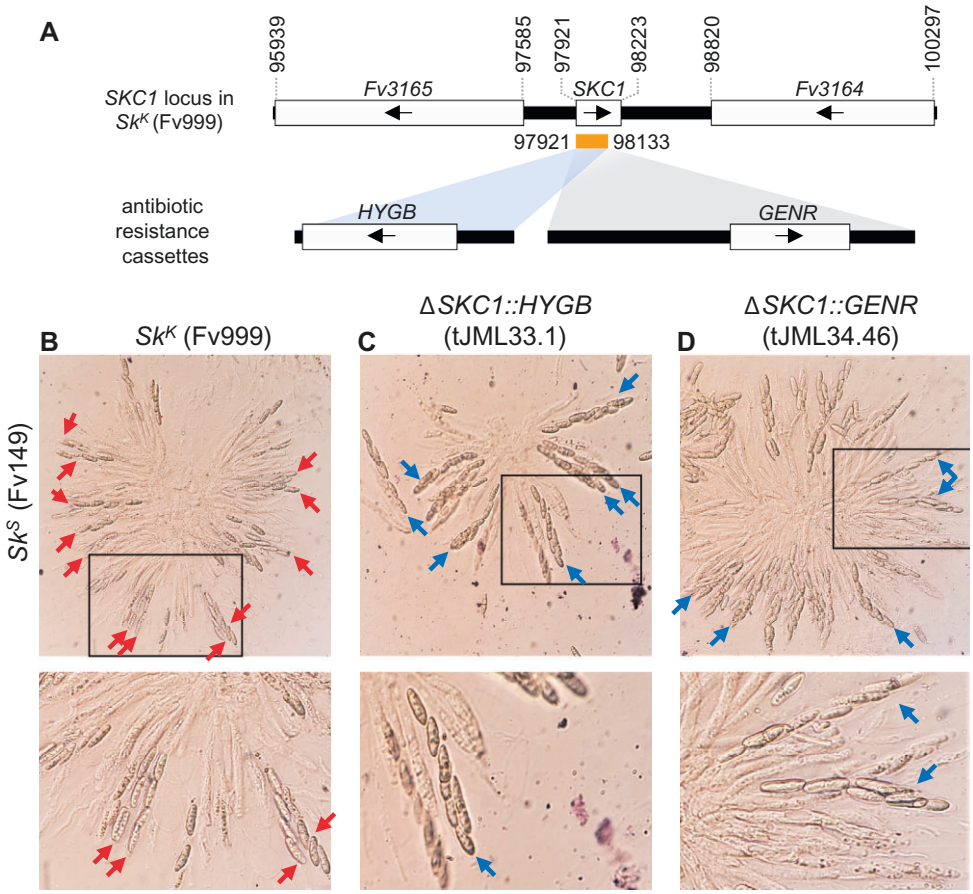

Fig. 1. Deletion of *SKC1* eliminates spore killing. a) A diagram of the *SKC1* deletion strategy is shown. Coding regions are represented by white rectangles. Promotor, terminators, untranslated sequences, and intergenic sequences are shown as black bars. Intron locations are not indicated. *Fv3165* and *Fv3164* are *SKC1*-flanking genes. *SKC1* coding sequences span positions 97,921 through 98,223. The deleted region (orange bar) includes the *SKC1* coding sequences up to the predicted stop codon in the genomic sequence (97,921–98,133). The deleted region was replaced with *HYGB* to create Δ*SKC1::HYGB* and *GENR* to create Δ*SKC1::GENR*. Positions are according to GenBank KU963213.1. The diagram is drawn to scale and the orange bar represents 213 base pairs (bp). b) $Sk^S \times Sk^K$ produces 4-spored asci. c) $Sk^S \times$ Δ*SKC1::HYGB* produces 8-spored asci. d) $Sk^S \times$ Δ*SKC1::GENR* produces 8-spored asci. Unidirectional crosses were performed with Sk^S as the female parent. Red and blue arrows mark 4-spored and 8-spored asci, respectively.

hereafter referred to as spore killing, in the *skc1* mutant was restored by complementation with *SKC1*.

Multiple copies of SKC1 trigger RIP in *F. verticillioides*

To investigate the cause of the inconsistent spore killing complementation phenotypes of Addback-A and Addback-B, we generated genome sequence data for the 3 addback strains. This analysis revealed that all 3 strains lacked *HYGB* (Supplementary Fig. 4), which is consistent with successful replacement of Δ*SKC1::HYGB* deletion construct with *SKC1* in each strain. Furthermore, all 3 strains had *GENR* (Supplementary Fig. 5), which is consistent with our use of *GENR* in the addback transformation procedure. In addition, all 3 strains possess *SKC1*, which was absent in their progenitor strain, the *skc1* mutant (Supplementary Fig. 6). However, the number of *SKC1*-specifc reads present in the genome sequence datasets of the addback strains suggests that each genome contained more than 1 copy of *SKC1* (Supplementary Fig. 6). Because our PCR-based genotyping assays indicated that the Sk^K locus of each addback strain had only 1 copy of *SKC1* (Supplementary Fig. 3), the additional copy(ies) of *SKC1* must have been located at an ectopic location(s).

Repeat-induced point (RIP) mutation occurs in some ascomycetous fungi during a cross when 1 parent contains 2 or more copies of a DNA sequence and results in the presence of multiple C-to-T transitions in the repeated sequence in progeny (Leslie and Dickman 1991; Aramayo and Selker 2013; Gladyshev 2017). If the repeated sequence is a gene, RIP can render all copies nonfunctional. Given the multiple copies of *SKC1* in the addback strains, RIP provides a possible explanation for the incomplete complementation phenotype of Addback-A and Addback-B. Therefore, we analyzed the genome sequences of 3 progeny from crosses of an Sk^S strain and Addback-A (progeny A3, A5, and A6) and 1 progeny from Addback-B (progeny B25). This analysis revealed that *SKC1* sequences in A5 and B25 had many C-to-T transitions, whereas *SKC1* sequences in A3 and A6 lacked such mutations (Table 3). The C-to-T transitions in *SKC1* sequences in A5 and B25 resulted in changes in the amino acid sequences as well as premature stop codons. Thus, RIP of *SKC1* sequences of some addback progeny and no RIP in other progeny is consistent with the incomplete complementation phenotype of Addback-A

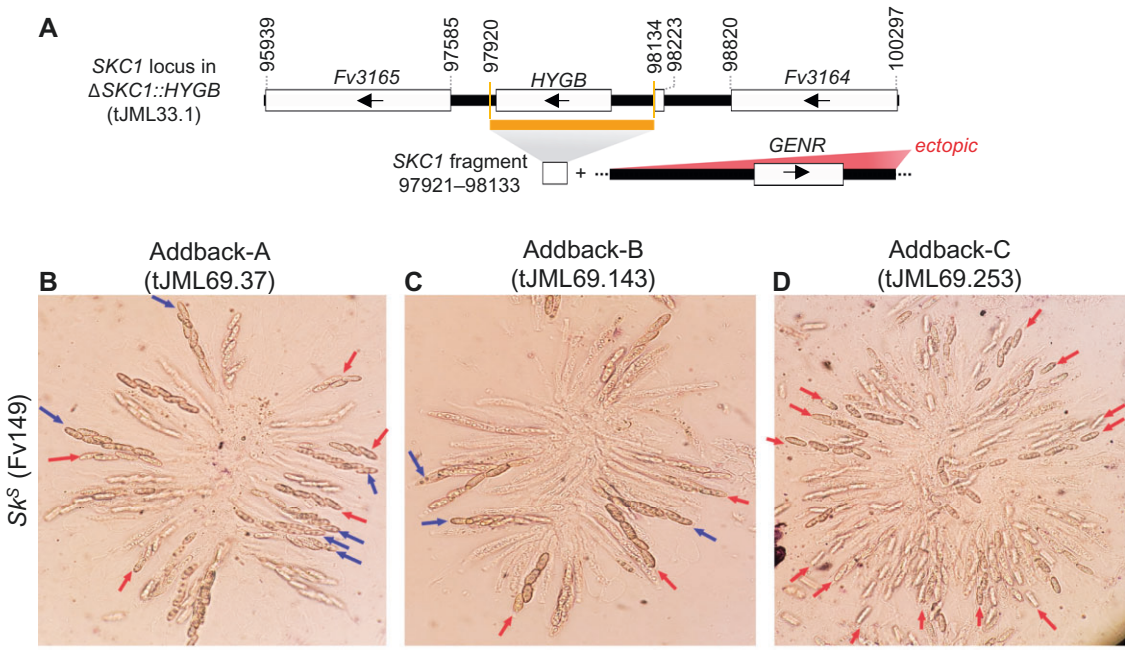

Fig. 2. *SKC1* restores spore killing to Δ*SKC1::HYGB*. a) A diagram of the cotransformation-based *SKC1* complementation strategy is shown. The procedure was designed to allow *HYGB* (marked by the orange bar) in Δ*SKC1::HYGB* to be replaced with the missing segment of *SKC1* (positions 97,921–98,133) while *GENR* integrates at an ectopic location in the genome. A portion of pGenNotI derived plasmid sequences was amplified along with the *GENR* cassette (dashed black line) for use in the transformation procedure. The diagram was drawn to scale. For reference, the orange bar represents 1,451 bp. Other style conventions are as in Fig. 1a. b) Sk^S × Addback-A produces a mix of 4-spored and 8-spored asci. c) Sk^S × Addback-B produces a mix of 4-spored and 8-spored asci. d) Sk^S × Addback-C produces 4-spored asci (8-spored asci were not observed). Unidirectional crosses were performed with Sk^S as the female. Red and blue arrows mark 4- and 8-spored asci, respectively.

and Addback-B. That is, C-to-T transitions that affect *SKC1* function are expected to block spore killing and result in asci with 8 ascospores, whereas the absence of C-to-T transitions are expected to allow spore killing to occur and result in asci with 4 ascospores.

SKC1 transcripts undergo A-to-I editing during sexual development

Previously, we examined transcript levels of 42 *SKC1*-linked genes during 6 stages of sexual development, from 2 h postfertilization to the early spore ejection stage (Pyle *et al.* 2016). We accomplished this by analyzing RNAseq datasets that had been generated from a cross between Sk^K (Fv999) and Sk^S (Fv149), where Sk^K served as female (Sikhakolli *et al.* 2012). A significant finding from this analysis was the discovery that *SKC1* transcripts are present at relatively high levels through all analyzed stages of sexual development. For example, of the 42 genes analyzed, *SKC1* transcripts were the most numerous at the first time point and the second most numerous at the last time point. The finding that *SKC1* transcript levels are relatively high even at early stages of sexual development raises the possibility that *SKC1* transcription is not tightly linked to sexual development.

To further examine *SKC1* expression, we performed strand-specific RNA sequencing on RNA isolated from 2 developmental stages of *F. verticillioides*: (1) vegetative tissue of an Sk^K after 4 days of growth on CA (mycelial dataset) and (2) perithecia from an Sk^S × Sk^K cross 20 dpf (perithecial dataset). Mapping RNA sequence reads from vegetative and perithecial tissue to the *SKC1* locus revealed that *SKC1* is bidirectionally transcribed (Fig. 3, a and b). Here, we define reads that matched the reference *SKC1* mRNA (GenBank KU963213.1) as "sense" sequences (Fig. 3, blue bars) and those that were complementary to the reference *SKC1* mRNA as "antisense" sequences (Fig. 3, red bars).

The ratio of antisense to sense *SKC1* sequences was higher in mycelia than perithecia (Fig. 3, a and b). Thus, we used the mycelial dataset to derive a model of antisense *SKC1* transcription. Specifically, we predicted that 2 antisense *SKC1* transcripts, antisense-SKC1a and antisense-SKC1b (with intron), are transcribed from *SKC1*. Our model posits that the transcripts possess the same +1 site and transcriptional cleavage site, but they differ with respect to intron sequence that is removed from antisense-SKC1a and retained in antisense-SKC1b (Fig. 3a and Supplementary Fig. 7a). Results of an RT-PCR analysis of RNA isolated from *F. verticillioides* mycelia were consistent with the existence of both antisense-SKC1a and antisense-SKC1b (Supplementary Fig. 7, b–d). While the role these transcripts play in spore killing is unclear, both lack obvious coding sequences, which suggests that they are noncoding RNAs.

The ratio of sense to antisense *SKC1* sequences was higher in perithecia than mycelia (Fig. 3, a and b). Thus, we used the perithecial dataset to derive a model of sense *SKC1* transcription. By examining RNA sequence coverage levels across *SKC1*, we identified a transcript called sense-SKC1 that included +1 site, an intron, a transcriptional cleavage site, a translational start codon, and a UAG stop codon (Fig. 3b). However, manual inspection of aligned sequences revealed many reads that spanned the stop codon of sense-SKC1 but some reads had UGG, which is a codon sequence for tryptophan, rather than the stop codon sequence UAG. The change in sequence from UAG to UGG is evidence of A-to-I RNA editing (Bian *et al.* 2019). Using both the mycelial and perithecial datasets, we then examined all sense RNA sequence reads and calculated the percentage of sequences showing evidence of A-to-I editing (Table 4). There was evidence for A-to-I editing in 84% of reads from perithecia but only 0% of reads from mycelia (Table 4). These results suggest that the A-to-I edit in sense-SKC1 is specific to sexual development. We

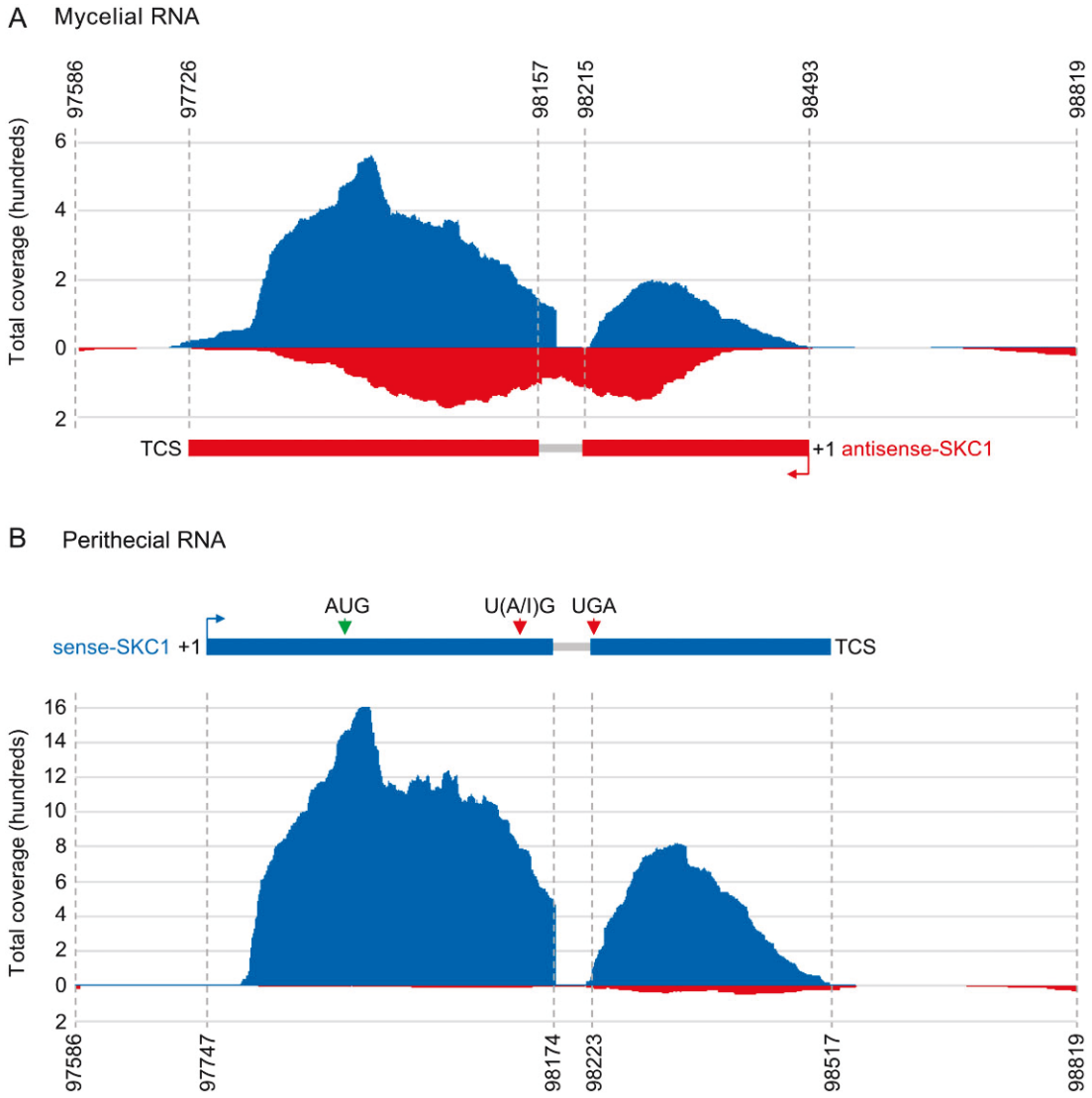

Fig. 3. *SKC1* is bidirectionally transcribed. a) RNA sequences from the mycelial dataset were mapped to an *SKC1*-containing reference sequence using custom python scripts (Supplementary Fig. 15). The chart depicts RNA coverage levels for positions 97,586 through 98,819 of the previously defined 102-kb *SKC1* locus (GenBank KU963213.1). Blue and red vertical bars indicate coverage levels for the reference ("sense") strand and nonreference ("antisense") strand, respectively. Antisense coverage levels were used to predict the location of a +1 site, 2 exons, an intron, and a transcriptional cleavage site (TCS) for a transcript called antisense-SKC1a (see *Materials and methods*). A variant transcript called antisense-SKC1b results when the intron is retained in the antisense transcript. b) RNA sequences from the perithecial dataset were mapped to an *SKC1*-containing reference sequence. Sense coverage levels were used to predict the location of a +1 site, 2 exons, an intron, a TCS, a start codon, and 2 stop codons for transcripts called sense-SKC1a and sense-SKC1b. The transcripts are nearly identical, except that codon 71 is a UAG codon in sense-SKC1a and a UIG codon in sense-SKC1b.

Table 4. RNA editing during sexual development.

RNAseq dataset	Total[a]	UAG[b]	UGG[c]	A → I[d]
Vegetative (Mycelia)	215	215	0	0.0%
Perithecial (Perithecia)	997	161	835	83.8%

[a] The number of sense RNA sequencing reads that map to the *SKC1* A-to-I edit site in the mycelial or perithecial datasets.
[b] Number of UAG reads.
[c] Number of UGG reads.
[d] Percentage of A-to-I editing (UGG/[UAG + UGG]). One read was UCG in the perithecial dataset (161 + 835 + 1 = 997). Three reads had multiple base changes across UAG and thus were ignored.

confirmed the read mapping results by sequencing RT-PCR products that spanned the UAG codon in sense-SKC1 (Fig. 4, b and c). As expected, transcripts with the A-to-I edit were absent in mycelia and present in perithecia. In contrast to the A-to-I edit, analysis of the RT-PCR amplicon sequence revealed that the *SKC1* intron in sense *SKC1* transcripts was absent from both mycelia and perithecia (Fig. 4c). Overall, these data suggest that *SKC1* is transcribed to produce at least 2 sense transcripts: transcript sense-SKC1a, which has the originally predicted UAG stop codon, and transcript sense-SKC1b, which has the UGG, tryptophan coding codon, formed by A-to-I editing and a UGA stop codon formed after excision of the intron (Figs. 3b and 4a).

While designing PCR primers for analysis of sense *SKC1* transcripts by RT-PCR, we discovered repeated elements within the putative 5′ untranslated regions (UTR) of sense-SKC1a and sense-SKC1b (Fig. 4a). Element ACACAA is repeated 5 times within the first 116 nucleotides of the transcripts. The other repeat is 21

A Sense-SKC1a and sense-SKC1b sequence model

5'**CAGGCGUCCAUCUUCUGUCUU**CUGUUUACUUUCUUCCUUACACACAAUUCCAUCAAUCCACUACACA
AUUCCAUCAAUCCACUACACAAUUCCAUCAAUCCACUACACAAACACAAGUUGUCUAUCAAGAAAUCAU
CUCUCAUUCUAUCUCCCAGAUCACCAAUCAAUACAGCCAUGUCUACCAACUCAGACACCAUGCCUG**GCG**
UUAUCCUCCACCUUUCAUCAGAUGAUCUUGAUGUUUUGCUUGAUAAGAAGCUACAGCCUAUUUACACUA
UGCUGGCUACUAUUAUCAAGAAACUUGAUGAUCUUACCGACCGUGUUGAGGCAGUUGAAGGCCUGGCGA
AAAAGAUCCCGGACAUGGAAGUCGAUAUCCAUUCUCAAGACUAGAGGCUGAAGAAGAUUGAGGCGCAGC
UUUUGUCCAGGACAUGGUUAGUUCGUUCUCUAGAAUGAAUAAUUAUAUGCUAAUACCAAGACAGAUUCA
AGACUUUCUUUACGCUCAUUCCCAUGUCGGGCUGGACCUUUGAAGAGGCGAUCGUGACAAACGCCGAGG
CGAUGGUUGGGUGCGCUGAUGGAGGUGGUGGAGAGAUGUCAUAUGGGCGUGGUUGGAGGUGAGGGACAG
UAAAUUUGGGCACUGUACCCUACCUGAGUACUAUGCCUGACGCAGUAUUCAUAUGGACAUGCACUCAUU
CUUGUACGUCAUGAUAAGUCCAUCCAUCAUAUCAUAG**ACUACCCCGCCAUGAACUGGAG**UGCUUGACUC
UAUCUCGGCGGCUU-3'

B RT-PCR analysis of sense *SKC1* transcripts

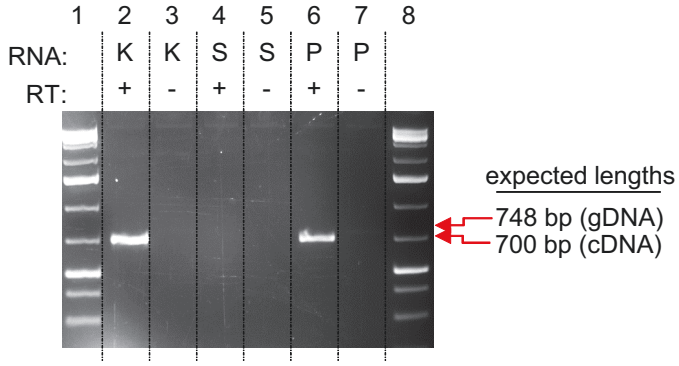

C Sanger sequencing analysis of sense *SKC1* RT-PCR products

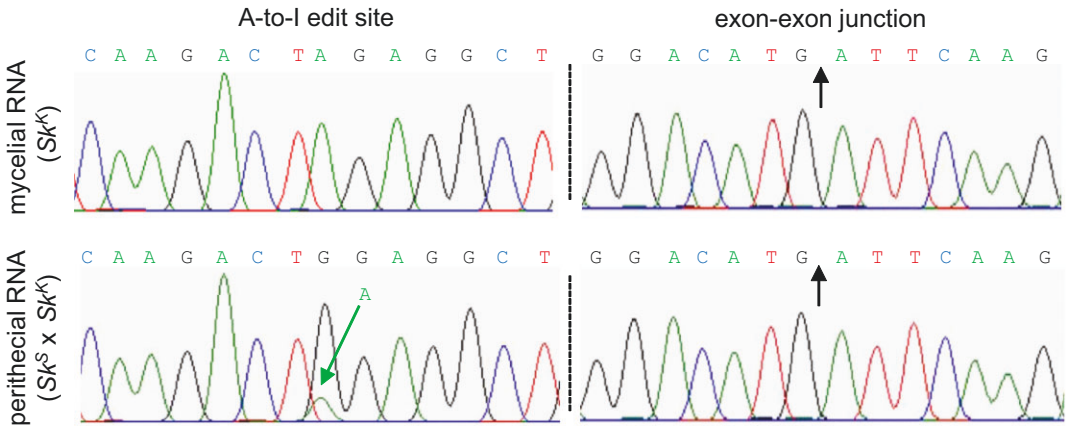

Fig. 4. Fungal A-to-I mRNA editing of *SKC1*'s UAG stop codon to UIG occurs in perithecia. a) The sequence of sense-SKC1 is shown. Two sequence motifs of unknown function are present in the 5′ UTR: ACACAA (double underline) and ACACAAUUCCAUCAAUCCACU (single underline). The locations of a putative start codon (green), UAG stop codon (blue), and intron (gray) are highlighted. The sense-SKC1b sequence contains a single nucleotide difference relative to the sense-SKC1a sequence: the UAG stop codon has been edited to a UIG tryptophan codon. The stop codon for sense-SKC1b is the UGA codon (red highlight) formed by intron removal. b) *SKC1* RT-PCR products were analyzed by gel electrophoresis. Lanes 1 and 8 contain 0.5 μg of GeneRuler 1 kb Plus DNA Ladder (ThermoFisher, 10787018). RNA: K, S, and P indicate that total RNA came from Sk^K-vegetative tissue, Sk^S-vegetative tissue, or $Sk^S \times Sk^K$ perithecia (see *RNA isolation*). RT: "+" indicates that reverse transcriptase was included in the first strand synthesis reaction, while "–" indicates that the enzyme was omitted from the first strand synthesis reaction. c) Sequence analysis of the RT-PCR products in lanes 2 (top) and 6 (bottom) of (b). The chromatogram segments span either the A-to-I edit site (left) or the exon–exon junction (right). The green arrow in the bottom left panel highlights UAG to UIG editing detected only in perithecial tissue. Only the "A" peak is present in vegetative tissue. The black arrows highlight the exon–exon junction as expected in vegetative and perithecial tissue.

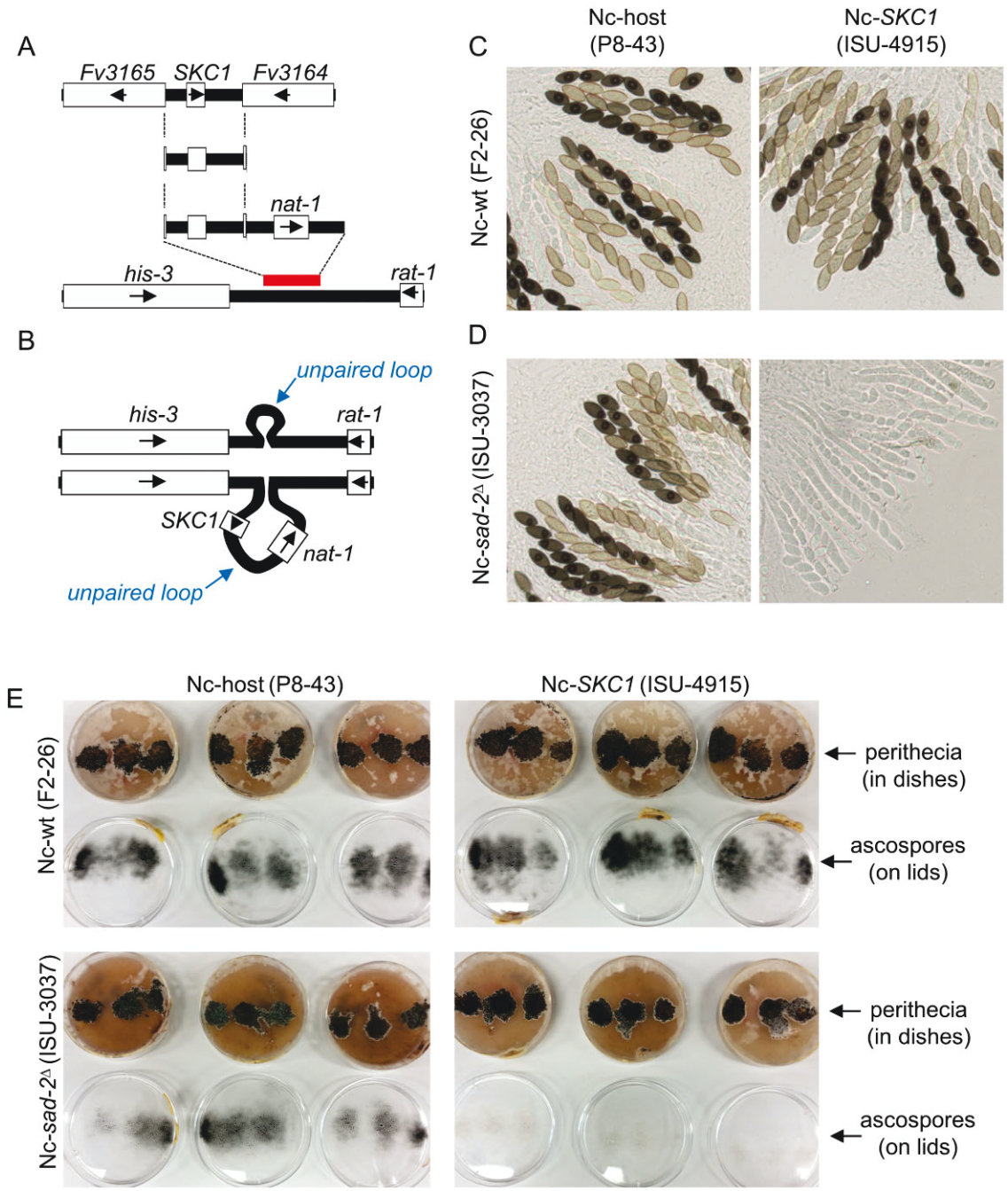

Fig. 5. *SKC1* restricts ascus development in *N. crassa*. a) A DNA fragment containing *SKC1*, *SKC1*'s intergenic flanks, and short segments of *SKC1*'s flanking genes' coding sequences were ligated to a nourseothricin resistance cassette (*nat-1*) and used to replace a 919-bp segment of intergenic DNA (red bar) between the *his-3* and *rat-1* genes on chromosome I in *N. crassa*. b) The *SKC1* gene is unpaired during meiosis in meiotic cells of a Nc-wt × Nc-*SKC1* cross. This phenomenon is symbolized by the "unpaired loop" in the diagram of an alignment between the his-3 locus of a wt parent and the his-3 locus of an *SKC1* parent. The *SKC1* gene is silenced during meiosis by MSUD because it is found within this unpaired loop. c) Nc-wt × Nc-host crosses and Nc-wt × Nc-*SKC1* crosses produce 8-spored asci. "Host" is the transformation host used for transformation with various *SKC1*-containing transgenes. d) Nc-*sad-2*$^{\Delta}$ × Nc-host crosses produce 8-spored asci while Nc-*sad-2*$^{\Delta}$ × Nc-*SKC1* crosses produce underdeveloped and/or aborted asci. e) Culture plates and lids for 4 types of crosses are shown. In *N. crassa*, mature spores are shot upwards by the perithecia and stick to the lids of culture plates. The 3 "black" circular shapes in each culture dish are masses of perithecia. The 3 diffuse black circular areas on the culture lids are spores that have collected on the lids. The lids have been removed from the culture plates to allow a qualitative comparison of perithecia and spore levels. The images show that, despite producing perithecia at levels that are roughly equivalent to the 3 control crosses (i.e. Nc-wt × Nc-host, Nc-wt × Nc-*SKC1*, and Nc-*sad-2*$^{\Delta}$ × Nc-host), Nc-*sad-2*$^{\Delta}$ × Nc-*SKC1* crosses produced few spores.

nucleotides long, contains the first repeat, and is found 3 times within the first 104 nucleotides of each transcript (Fig. 4a). As these repeats occur in the 5′ UTR of *SKC1*, they do not impact Skc1 protein sequence.

SKC1 disrupts ascospore development in *N. crassa*

To determine if *SKC1* can cause spore killing in other fungi, we inserted *F. verticillioides SKC1* into the genome of *N. crassa* (Fig. 5a). During meiosis in *N. crassa*, genes present in unpaired DNA are

repressed by a process called meiotic silencing by unpaired DNA (MSUD) (Aramayo and Selker 2013; Hammond 2017). Thus, we expected *SKC1* to be silenced when wild-type *N. crassa* (Nc-wt) was crossed with an *N. crassa* strain with *SKC1* (Nc-*SKC1*) because *SKC1* would be unpaired in such crosses. Indeed, asci from Nc-wt × Nc-*SCK1* crosses had the same number of ascospores as asci from crosses of 2 Nc-wt strains. To overcome MSUD, we crossed Nc-*SKC1* with an *N. crassa* strain (Nc-*sad-2*$^{\Delta}$) in which MSUD was suppressed (Shiu *et al.* 2006). In Nc-*sad-2*$^{\Delta}$ × Nc-*SCK1* crosses, ascus development stalled and/or aborted in most perithecia and only a few viable ascospores formed (Fig. 5, d and e and Supplementary Fig. 8a). In Nc-*sad-2*$^{\Delta}$ × Nc-wt crosses, by contrast, the vast majority of asci and ascospores developed to maturity and produced viable ascospores. To determine if *SKC1* is transmitted in a biased manner to the few viable ascospores produced by the Nc-*sad-2*$^{\Delta}$ × Nc-*SCK1* cross, we examined 32 offspring for the presence of *SKC1*. Nineteen of the offspring carried the *SKC1* allele, which, according to a simple chi-square test, is consistent with a 50% transmission rate. Together, these results indicate that *SKC1* restricts both ascospore and ascus development in *N. crassa* but also that, among the small number of viable ascospores that are formed, *SKC1* is not inherited in a biased manner.

SKC1 transcripts undergo A-to-I editing in a heterologous system

We also examined *SKC1* transcripts in *N. crassa* for evidence of A-to-I editing of the UAG stop codon. To do this, RNA recovered from perithecia from an Nc-*sad-2*$^{\Delta}$ × Nc-*SKC1* cross was used as a template to amplify and then sequence *SKC1* transcripts. The analysis indicated that some *SKC1* transcripts had the original stop codon sequence (UAG), while others had the edited sequence (UIG) (Fig. 6a). The analysis also revealed that the intron sequence was absent in *SKC1* transcripts in *N. crassa* regardless of whether the stop codon sequence was edited (Fig. 6b). These results provide evidence that *SKC1* transcripts undergo A-to-I editing and intron processing in *N. crassa* in the same manner as in *F. verticillioides*.

Codon change required for spore killing

The A-to-I editing of the *SKC1* transcript observed in both *F. verticillioides* and *N. crassa* raises the question: is the change in the codon sequence from UAG to UIG required for spore killing? To address this in *F. verticillioides*, we complemented the *skc1* mutant with a variant of *SKC1* in which the stop codon sequence was changed from TAG to TAA (SKC1$^{TAG>TAA}$) (tJML56.208) (Fig. 7a). We rationalized that the SKC1$^{TAG>TAA}$ transcript could undergo A-to-I editing but that the edit from UAA to UGA would result in a stop codon that would prohibit production of the 84 amino acid protein (Skc1b).

PCR and genome sequence analysis of the *skc1* mutant complemented with *SKC1*$^{TAG>TAA}$ (transformant Fv-SKC1$^{TAG>TAA}$) revealed that a single copy of *SKC1*$^{TAG>TAA}$ had replaced *HYGB* and that additional copies of *SKC1*$^{TAG>TAA}$ had integrated elsewhere in the genome (Supplementary Figs. 9 and 10). We removed the ectopic copies of *SKC1*$^{TAG>TAA}$ through meiotic reassortment by crossing transformant Fv-SKC1$^{TAG>TAA}$ with *Sk*^{S} strain Fv149. Genome sequence analysis of 2 of the resulting progeny, Offspring-C11 (tJML56.208 P11) and Offspring-C37 (tJML56.208 P37) revealed that both had only a single copy of the *SKC1*$^{TAG>TAA}$ gene that was positioned at the native *SKC1* locus and did not harbor any mutations indicative of RIP (Supplementary Fig. 11). Crosses of Offspring-C11 or Offspring-C37 with *Sk*^{S} strain Fv149 yielded asci with 8 ascospores, which indicated an absence of spore killing (Fig. 7c). These results provide evidence that the A-to-I editing that changes the stop codon (UAG) of the *SKC1* transcript to a tryptophan-specifying codon (UIG) is required for spore killing in *F. verticillioides*. This in turn indicates that transcript sense-SKC1b is required for spore killing but sense-SKC1a is not required.

To address the role of A-to-I editing of the *SKC1* stop codon in *N. crassa*, we introduced 2 variants of the *SKC1* gene into the fungus. In the first variant, we changed the stop codon sequence to TAA (*SKC1*$^{TAG>TAA}$), as described above for *F. verticillioides*. In the second variant, the stop codon sequence was changed from TAG to TGA (*SKC1*$^{TAG>TGA}$). For *SKC1*$^{TAG>TGA}$, we rationalized that transcripts could not undergo A-to-I editing because the target adenosine had been changed to guanine. In Nc-*sad-2*$^{\Delta}$ × Nc-*SKC1*$^{TAG>TGA}$ and Nc-*sad-2*$^{\Delta}$ × Nc-SKC1$^{TAG>TAA}$ crosses, ascus and ascospore development was not restricted, indicating that both *SKC1*$^{TAG>TGA}$ and *SKC1*$^{TAG>TAA}$ did not kill ascospores or interfere with their development (Fig. 6c and Supplementary Fig. 12).

To further refine the sequence that is responsible for spore killing, we generated an *N. crassa* strain with a third *SKC1* gene variant (*SKC1*$^{TAG>TGG}$), in which the stop codon sequence was changed from TAG to the tryptophan codon sequence TGG. In Nc-*sad-2*$^{\Delta}$ × Nc-*SKC1*$^{TAG>TGG}$ crosses, ascus and ascospore development were restricted in the same manner as in Nc-*sad-2*$^{\Delta}$ × Nc-*SKC1* crosses (Fig. 6, c and d). Together the results of the *SKC1* variant expression in *F. verticillioides* and *N. crassa* indicate that the absence of the stop codon at position 383 of the *SKC1* transcript is required for spore killing, and that a mixture of edited and unedited transcripts is not required for spore killing.

Distribution, phylogenetic relationships, and location of *SKC1* in *Fusarium*

To investigate the distribution of *SKC1* in *Fusarium*, we used BLASTn analysis of an inhouse database with genome sequences of 186 species representing all 23 multispecies lineages (species complexes) of the genus (Kim *et al.* 2020; Geiser *et al.* 2021). With *SKC1* as query, we detected 22 homologs in 19 species from 6 closely related species complexes: the *Fusarium burgessii* (Burgessii), *Fusarium newnesense* (Newnesense), *Fusarium nisikadoi* (Nisikadoi), *Fusarium oxysporum* (Oxysporum), *Fusarium redolens* (Redolens), and *Fusarium fujikuroi* (Fujikuroi) species complexes (Fig. 8). The 6 species complexes constitute a monophyletic lineage within *Fusarium*, however, within most of these complexes the presence of *SKC1* was discontinuous. For example, our *Fusarium* genome sequence database includes over 40 species within Fujikuroi, but *SKC1* was detected in only 12 of the species, including *F. verticillioides*. In the database used for this analysis, most species were represented by a single genome sequence. Therefore, a lack of detection of *SKC1* in a genome sequence could be because the species lacks *SKC1* or because the sequence was from an *Sk*^{S} strain of a species that has *SKC1*. With 1 exception, all species in which *SKC1* was detected had only 1 copy of the gene per genome sequence. The exception was *Fusarium foetens*; the 1 genome sequence examined had 3 *SKC1* paralogs. Two strains of *F. oxysporum* had *SKC1*, but the *SKC1* sequences from the 2 strains exhibited a relatively high level of divergence (Fig. 8).

MP and ML analysis resolved the 23 *SKC1* homologs into 4 clades (Fig. 8). The *SKC1* MP and ML trees mirrored recently reported *Fusarium* species trees (Kim *et al.* 2020; Geiser *et al.* 2021) in some respects but had some noteworthy differences. First, unlike species in the species trees, some *SKC1* sequences from the same species complex were more distantly related to one another

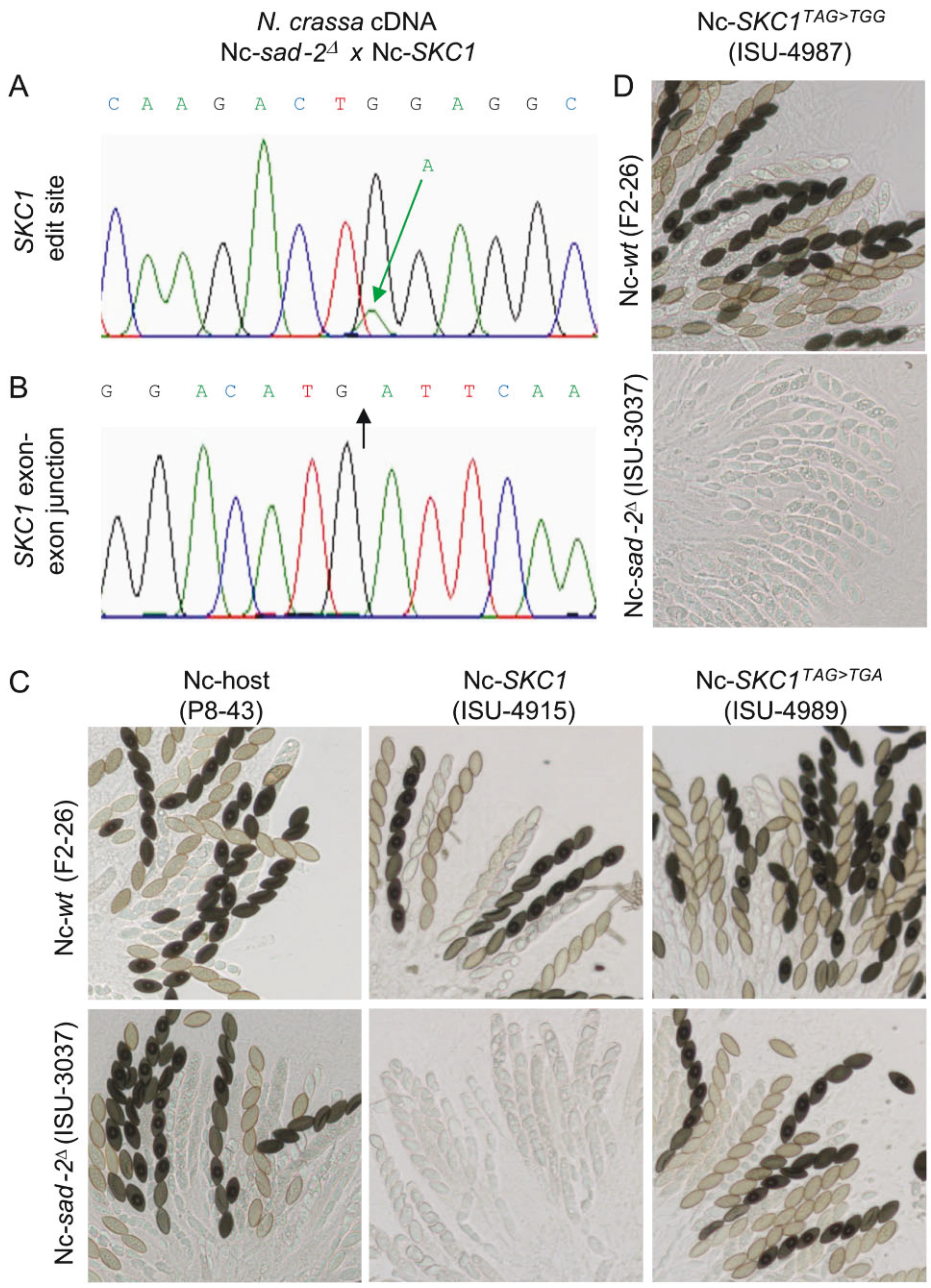

Fig. 6. *SKC1* function in *N. crassa* requires A-to-I mRNA editing. a) Sequence of an *SKC1* RT-PCR product amplified from total RNA of Nc-*sad*-2^{Δ} × Nc-*SKC1* perithecia (10 dpf). The chromatogram shows a major "G" peak and a minor "A" peak at the edit site, indicating that A-to-I editing of *SKC1*'s UAG stop codon occurs in *N. crassa* as it does in *F. verticillioides*. b) Sequence of the same amplicon described in (a) spaning the *SKC1* exon–exon junction. The chromatogram shows that the exon–exon junction forms properly in *N. crassa*. c, top row) Nc-wt × Nc-host, Nc-wt × Nc-*SKC1*, and Nc-wt × Nc-*SKC1*$^{TAG>TGA}$ crosses produce 8-spored asci. c, bottom row) Nc-*sad*-2^{Δ}× Nc-host and Nc-*sad*-2^{Δ} × Nc-*SKC1*$^{TAG>TGA}$ crosses produce 8-spored asci, while Nc-*sad*-2^{Δ} × Nc-*SKC1* crosses produce underdeveloped/aborted asci. d) Crosses of Nc-wt × Nc-*SKC1*$^{TAG>TGG}$ produce 8-spored asci, while Nc-*sad*-2^{Δ} × Nc-*SKC1*$^{TAG>TGG}$ crosses produce underdeveloped/aborted asci.

than sequences from different complexes. For example, in the *SKC1* tree, clade 1 included sequences from both the Fujikuroi and Newnesense complexes, while clade 2 included sequences from the Fujikuroi, Nisikadoi, and Oxysporum complexes. Likewise, the relationships of *SKC1* sequences from species of the Fujikuroi complex did not always correlate with relationships of the species within the complex. This was apparent when the *SKC1* trees were considered in the context of the 3 major clades (African, American, and Asian) into which members of the Fujikuroi complex have been resolved in previous phylogenetic analyses (O'Donnell *et al.* 1998; Kim *et al.* 2020). For example, in the *SKC1* tree, sequences from the African clade species *F. thapsinum* grouped in Clade 2 and were relatively distantly related to sequences from other African clade species (i.e. *Fusarium musae*, *Fusarium secorum*, *Fusarium udum,* and *F. verticillioides*), which grouped in Clade 1 (Fig. 8). Furthermore, the 3 *SKC1* homologs from *F. foetens* were relatively distantly related to one another; each was resolved in a different *SKC1* clade (Fig. 8).

The relative genomic location of the *SKC1* homologs in each *Fusarium* strain was assessed by examining their flanking genes

(Supplementary Table 2). Here, we determined that *SKC1* homologs occurred at 11 different locations (Fig. 8). The locations were not necessarily correlated with the 4 major *SKC1* clades shown in Fig. 8 or with species complexes. For example, 4 of the 6 *SKC1* homologs in Clade 2 occurred at location 7, whereas the 11 *SKC1* homologs in Clade 1 occurred at any 1 of 6 locations. Further, *SKC1* homologs from members of the Fujikuroi complex occurred at any 1 of 7 locations, and each of the 3 *F. foetens* paralogs occurred at a different location. *SKC1B* of *F. foetens*, a member of the Oxysporum complex, is most closely related to and occurs in the same location (9) as the 2 *F. oxysporum SKC1* homologs, whereas *F. foetens SKC1A* and *SKC1C* were more distantly related to and at different locations (8 and 11, respectively) than the *F. oxysporum SKC1* homologs.

It is noteworthy that of the 20 *Fusarium* species with *SKC1*, only the *F. musae* homolog was identical in sequence to *F. verticillioides SKC1* (Supplementary Figs. 13 and 14). Even though *SKC1* homologs from other species differed from the *F. verticillioides*

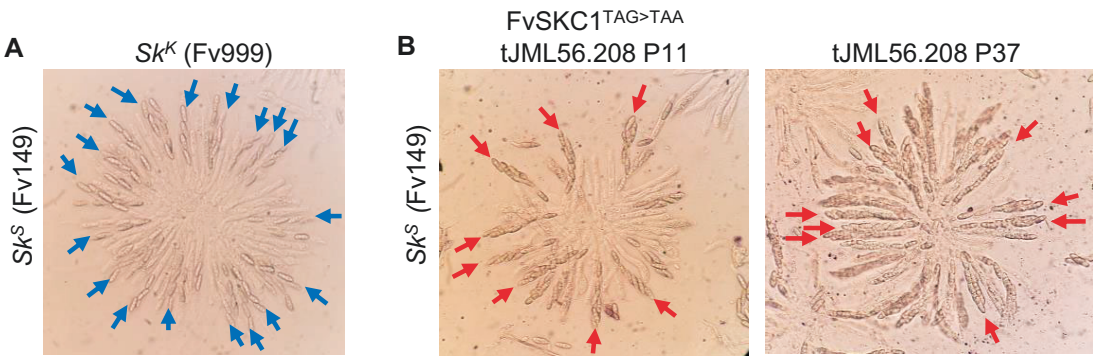

Fig. 7. Sense-SKC1b is required for spore killing. a) Control Sk^S (Fv149) × Sk^K (Fv999) cross produced 4-spored asci. b) Sk^S × Fv-SKC1$^{TAG>TAA}$ C-11 and Sk^S × Fv-SKC1$^{TAG>TAA}$ C-37 crosses produced 8-spored asci. Unidirectional crosses were performed with Sk^S (Fv149) as the female strain. Red and blue arrows mark 4- and 8-spored asci, respectively.

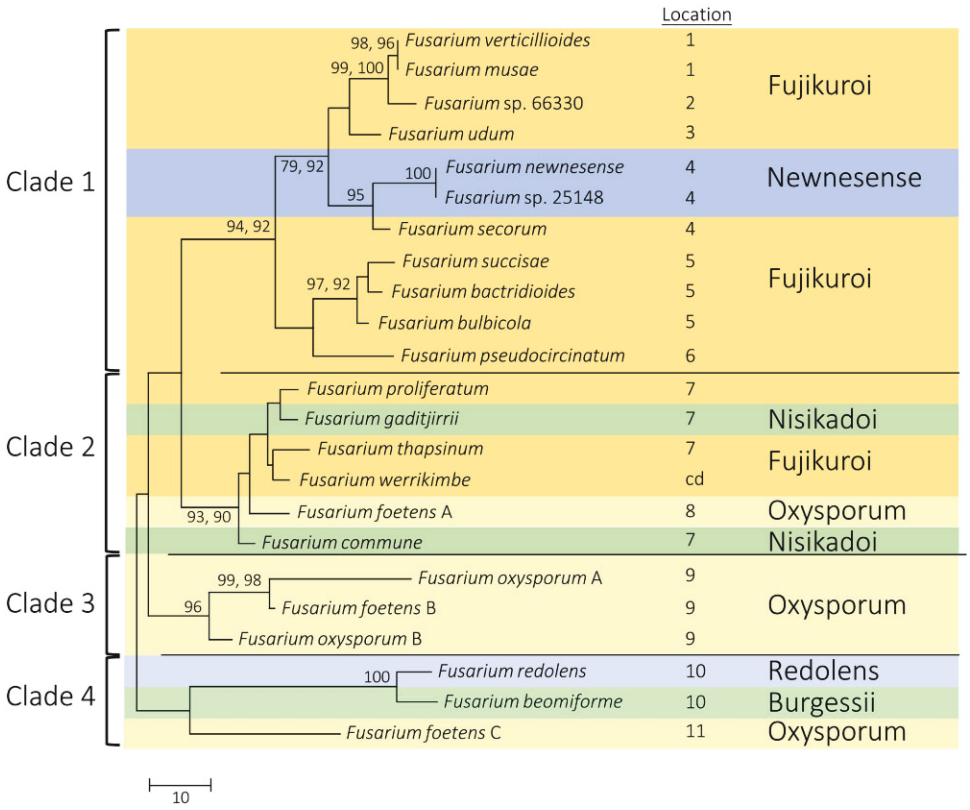

Fig. 8. Genealogy of *Fusarium SKC1* homologs inferred by MP and ML analysis of nucleotide coding sequences. Statistical support for branches within the phylogenetic tree were generated by bootstrap analysis with 500 pseudoreplicates and are indicted by numbers near the internodes: # = MP, ML. A single number indicates that the bootstrap values were the same. Major clades are demarked by horizontal lines. *F. foetens* A–C indicate 3 *SKC1* paralogs in one strain. *F. oxysporum* A and B refer to 2 different *SKC1* homologs from 2 different strains, Fo4287 (NRRL 34936) and Foii5 (NRRL 54006). Location number refers to different genomic locations of the *F. verticillioides* homologs of the genes flanking the *SKC1* homologs. The *Fusarium* species complex of each strain is indicated on the right and is highlighted by a unique background color in the tree (i.e. Fujikuroi is an abbreviation for *F. fujikuroi* specie complex). cd = could not determine because *SKC1* was present on a small contig that did not include any flanking genes.

homolog at numerous positions of both the nucleic acid and predicted amino acid sequences, all homologs were conserved with respect to the TAG stop codon (Supplementary Fig. 13). This raises the possibility that the *SKC1* homologs in the other species undergo A-to-I RNA editing in the same manner as in *F. verticillioides*.

Discussion

Spore-killing meiotic drive elements, or gene drives, in species of the Sordariomycetes have been a topic of study for 4 decades. However, genes responsible for spore killing as well as resistance to killing, have been identified and characterized only within the last decade. Gene drives have the potential to revolutionize efforts to limit mycotoxin contamination and plant disease by providing farmers with a highly efficient, targeted approach to either kill or neutralize problematic organisms (Wedell *et al.* 2019; Gardiner *et al.* 2020). Like any new technology, effective use of gene drives to control agricultural problems will require a thorough understanding of the process. Some important questions about gene drives that require answers are, what genes confer gene drive/killing in fungi; how do natural gene drives function; do genes linked to gene drives impact competition among isolates in the environment or selection by host plants? In the current study, we identified *SKC1* as a gene within the *Sk* locus that confers spore killing in *F. verticillioides*, a fungus that contaminates maize with the carcinogenic mycotoxins fumonisins worldwide. We also used multiple approaches to elucidate how *SKC1* confers spore killing.

Our results demonstrated that deletion of *SKC1* eliminated the *Sk*-mediated spore killing, allowing production of 8 ascospores per ascus during sexual development, while complementation of the deletion mutant restored spore killing. Transcriptional profiling of vegetative and sexual tissue indicated differential regulation of *SKC1* and formation of 4 distinct *SKC1* transcripts: 2 sense transcripts, of which one occurred exclusively in sexual tissue; and 2 antisense transcripts that occurred almost exclusively in vegetative tissue. The single nucleotide difference between the 2 sense transcripts occurred within the second position of predicted *SKC1* stop codon (TAG) based on the genomic sequence of the gene. Transcript sense-SKC1a has the stop codon (UAG) sequences, whereas transcript sense-SKC1b has the codon UGG instead of the stop codon. As a result, sense-SKC1a is predicted to encode a 70-aa protein (Skc1a) and sense-SKC1b is predicted to encode an 84-aa protein (Skc1b), which consists of Skc1a with a 14-aa extension at the carboxy terminal end.

The single-nucleotide difference between sense-SKC1a and sense-SKC1b is consistent with A-to-I mRNA editing, a posttranscriptional modification process that involves deamination of adenosine (A) to form inosine (I) (Bian *et al.* 2019). Ribosomes recognize I as a guanine (G), which can lead to a change in codon specificity and, therefore, a change in amino acid sequence. In *Fusarium graminearum* and *F. verticillioides*, thousands of A-to-I editing events have been documented specifically during sexual development, and in *F. graminearum* some of the editing events change protein function (Liu *et al.* 2016; Bian *et al.* 2019; Liang *et al.* 2021). In *N. crassa*, transcripts for the gene *rfk-1*, which is required for the meiotic drive element *Sk-2*, also undergo A-to-I mRNA editing exclusively in sexual tissue (Rhoades *et al.* 2019). In the current study, identification of the putative A-to-I editing of *SKC1* transcript raised the question, is spore killing induced by the edited *SKC1* (sense-SKC1b) transcript or the larger Skc1b protein? Protein structure predictions by Rosetta, as implemented on the Robetta server (Kim *et al.* 2004), indicate that the C-terminus of Skc1b models includes an alpha-helix extending 4–5 turns that is not present in Skc1a models. Because neither Skc1a nor Skc1b share sequence similarity to proteins of known function, it is not clear how the carboxyterminal alpha-helix of Skc1b could cause spore killing.

In the initial transcriptomics experiment, vegetative tissue was meant to serve as a negative control for *SKC1* expression, because we expected *SKC1* expression to occur only during sexual development. Consistent with this expectation, we did not observe any phenotypic differences between in the *skc1* mutant and the wild type during growth on/in solid or liquid media. Instead, we detected significant *SKC1* expression during vegetative growth, which, included 2 antisense transcripts. One possible role for the antisense transcripts could be to protect vegetative tissue by interfering with or repressing sense *SKC1* transcript function (Pelechano and Steinmetz 2013).

To shed light on the potential roles that the alternative forms of *SKC1* transcripts and/or proteins play in spore killing, we expressed a modified version of *SKC1* in *F. verticillioides* and 4 versions of *SKC1* in the model fungus *N. crassa*. These experiments revealed in both fungi that *SKC1* transcripts undergo A-to-I editing to form sense-SKC1b and that the sense-SKC1b transcript is required. In contrast to *F. verticillioides*, in *N. crassa SKC1* does not act as a meiotic driver in that only 50% of surviving progeny inherit *SKC1* and ascus developmental defects do not require a mixture of unedited and edited transcripts. In *F. verticillioides*, the presence of the Sk^K loci in almost 100% of surviving ascospores suggest that the loci also provide resistance to killing, similar to *Sk-1* in *N. crassa* (Svedberg *et al.* 2021). The failure of *SKC1* to drive in *N. crassa* suggests that resistance afforded by Sk^K in *F. verticillioides* is separate from *SKC1* or is dependent on *F. verticillioides*-specific spatial or temporal cues.

Our survey of genome sequences detected *SKC1* in species of 6 closely related *Fusarium* species complexes, indicating that Sk^K-mediated spore killing could be more widespread in the genus than reflected in the literature (Sidhu 1984; Raju 1994; Pyle *et al.* 2016). The presence of *SKC1* was discontinuous within most species complexes in which it was detected. However, given that Sk^S strains of *F. verticillioides* lack *SKC1* and that we examined only a single genome sequence of most species, the absence of *SKC1* in some genome sequences could reflect the presence of 2 genotypes (Sk^K and Sk^S) within a species rather than absence of *SCK1* in the species as a whole. Nevertheless, if *SKC1* was more widely distributed in *Fusarium* than indicated by the results of our survey, we expected that it would have been detected in at least some genomes representative of other species complexes, particularly if the frequency of *SKC1* in the species was similar to the frequencies observed in this study for strains of *F. verticillioides* (~50%) and *F. proliferatum* (~90%). Indeed, the GenBank database includes genome sequences for 19 strains of the species *F. fujikuroi*, but *SKC1* was not detected in any of them.

As far as we are aware, the spore killing phenotype has been reported in 3 *Fusarium* species: *F. verticillioides* (Kathariou and Spieth 1982), *F. subglutinans* (Sidhu 1984), and *F. proliferatum* (Raju 1994). In our survey, we did not detect *SKC1* in 8 genome sequences of *F. subglutinans*. It is possible that these 8 strains were Sk^S, which suggests that the frequency of Sk^K strains was lower than the 50% that we observed for *F. verticillioides*. Another possibility is that the spore killing system in *F. subglutinans* is distinct from the *SKC1*-mediated system in *F. verticillioides*. Yet another possibility is that the spore killing described by Sidhu (1984) occurred in *F. temperatum*, a species that was considered synonymous with

F. subglutinans prior to 2011 (Scauflaire *et al.* 2011). However, we did not detect *SKC1* in any of the 5 *F. temperatum* genome sequences included in our survey. In contrast to *F. subglutinans*/*F. temperatum*, we did detect *SKC1* in *F. proliferatum*, which indicates that the previously reported spore killing in this fungus (Raju 1994) could be mediated by *SKC1*. It is note-worthy that the species *F. siculi* and *F. hostae* have *SKC1* homologs that are likely to be non-functional because each contains premature stop codons (Supplementary Table 2). Translation of the shorter ORFs would result in proteins that are 22 and 29 amino acids shorter at the carboxy-terminus than Skc1a from *F. verticillioides*. Because all 3 premature stop codons are UAA, A-to-I editing would not be expected to lead to a longer ORF in transcripts because the codon formed from the editing would be UGA, which is also a stop codon.

The different genomic locations and relatively distant phylogenetic relationships of the 3 *SKC1* paralogs in *F. foetens* indicate that they did not arise from a recent gene duplication event. The presence of at least 2 paralogs could be the result of horizontal gene transfer (HGT). While *F. foetens* is a member of the Oxysporum complex, *SKC1A* is most closely related to homologs from members of the Fujikuroi and Nisikadoi complexes. If *SKC1A* was horizontally transferred to *F. foetens*, a member of one of these 2 complexes would be a likely donor. Likewise, branch conflicts between the *SKC1* tree (Fig. 8) and recently reported *Fusarium* species trees (Kim *et al.* 2020; Geiser *et al.* 2021) are consistent with HGT of *SKC1* within and among species complexes. For example, in the *SKC1* tree, sequences from 2 species of the Newnesense complex are nested within a clade of sequences from the Fujikuroi complex, which is consistent with HGT of *SKC1* from a member of Fujikuroi to an ancestor to the 2 Newnesense species. In support of this, the *SKC1* homologs in the 2 Newnesense species are located at the same relative genomic location (4) as the *SKC1* homolog in *F. secorum*, a member of Fujikuroi. Alternative explanations for conflicts also include incomplete lineage sorting of ancestral *SKC1* alleles or paralogs resulting from ancient duplication events (Proctor *et al.* 2013; Steenwyk *et al.* 2019). It is also possible that the multiple conflicts between the *SKC1* and species trees have resulted from a combination of these evolutionary processes. Together, the results of our survey and phylogenetic analyses of *SKC1* indicate a complex evolutionary history of the gene during divergence of at least 6 *Fusarium* species complexes. It remains to be determined whether such complexities have affected the ability of *SKC1* to confer spore killing. Ongoing experiments to determine whether *SKC1* homologs from other species can complement an *F. verticillioides skc1* mutant could provide further insight into the evolutionary history and functionality of the gene.

Data availability

Strains and plasmids are available upon request. The RNA sequencing datasets and the mutant genome sequences reported in this study have been deposited in NCBI's Sequence Read Archive (Leinonen et al. 2011) under BioProject accession number PRJNA768118 and the following: SRR16169787 (Δ*SKC1::HYGB*), SRR16169786 (Δ*SKC1::GENR*), SRR16169784 (Addback-A), SRR16169783 (Addback-B), SRR16169782 (Addback-C), SRR16169781 (Offspring-A3), SRR16169780 (Offspring-A5), SRR16169779 (Offspring-A6), SRR16169778 (Offspring-B25), SRR16169777 (Dataset: Mycelial), and SRR16169785 (Dataset: Perithecial). Strains Fv149 and Fv999 can be obtained from the Fungal Genetics Stock Center (McCluskey *et al.* 2010). *Fusarium* genome sequence data are available at GenBank and the accession numbers are listed in Supplementary Table 2.

Supplemental material is available at *GENETICS* online.

Acknowledgments

The authors dedicate this work to P.T. Spieth, S. Kathariou, and G.S. Sidhu, whose identification of Sk^K and early studies of the meiotic drive element made this work possible. We are grateful to Dr. John Leslie (Kansas State University; Fungal Genetics Stock Center) and Dr. Frances Trail (Michigan State University) who kindly provided Fv999 and Fv149. We thank Chris McGovern and Amy McGovern of the National Center for Agricultural Utilization Research for technical assistance. They also are thankful for the efforts of Joshua Burkhead (ISU graduate student), Elise Webber (ISU undergraduate student), and Gracie Abraham (ISU undergraduate student) for their efforts on characterizing the loss of drive in an early *SKC1* deletion mutant. This work was omitted from the manuscript because the mutant was later determined to have resulted from integration of multiple copies of the deletion vector at the native *SKC1* locus.

Funding

This project was supported by a grant from the National Science Foundation to TMH (MCB 1615626/2005295). JML, RHP, and DWB were supported by the United States Department of Agriculture, Agricultural Research Service Project Number 5010-42000-053-00D. Mention of trade names or commercial products in this article is solely for the purpose of providing specific information and does not imply recommendation or endorsement by the United States Department of Agriculture. The United States Department of Agriculture is an equal opportunity provider and employer.

Conflicts of interest

None declared.

Literature cited

Aramayo R, Selker EU. *Neurospora crassa*, a model system for epigenetics research. Cold Spring Harb Perspect Biol. 2013;5(10):a017921.

Basenko EY, Pulman JA, Shanmugasundram A, Harb OS, Crouch K, Starns D, Warrenfeltz S, Aurrecoechea C, Stoeckert CJ, Jr, Kissinger JC, *et al.* FungiDB: an integrated bioinformatic resource for fungi and Oomycetes. J Fungi. 2018;4:39.

Bian Z, Ni Y, Xu JR, Liu H. A-to-I mRNA editing in fungi: occurrence, function, and evolution. Cell Mol Life Sci. 2019;76(2):329–340.

Bravo Nunez MA, Nuckolls NL, Zanders SE. Genetic villains: killer meiotic drivers. Trends Genet. 2018;34(6):424–433.

Brockman HE, De Serres FJ. "Sorbose Toxicity" in Neurospora. Am J Bot. 1963;50(7):709–714.

Brown DW, Villani A, Susca A, Moretti A, Hao G, Kim HS, Proctor RH, McCormick SP. Gain and loss of a transcription factor that regulates late trichothecene biosynthetic pathway genes in *Fusarium*. Fungal Genet Biol. 2020;136:103317.

Campbell JL, Turner BC. Recombination block in the Spore killer region of *Neurospora*. Genome. 1987;29(1):129–135.

Carlson DB, Williams DE, Spitsbergen JM, Ross PF, Bacon CW, Meredith FI, Riley RT. Fumonisin B_1 promotes aflatoxin B_1 and N-

methyl-N'-nitro-nitrosoguanidine-initiated liver tumors in rainbow trout. Toxicol Appl Pharmacol. 2001;172(1):29–36.
Cavinder B, Sikhakolli U, Fellows KM, Trail F. exual development and ascospore discharge in *Fusarium graminearum*. J Vis Exp. 2012;61. https://doi.org/10.3791/3895. 10.3791/3895
Dalstra HJ, Swart K, Debets AJ, Saupe SJ, Hoekstra RF. Sexual transmission of the [Het-s] prion leads to meiotic drive in *Podospora anserina*. Proc Natl Acad Sci USA. 2003;100(11):6616–6621.
Desjardins AE, Brown DW, Yun SH, Proctor RH, Lee T, Plattner RD, Lu SW, Turgeon BG. Deletion and complementation of the mating type (*MAT*) locus of the wheat head blight pathogen *Gibberella zeae*. Appl Environ Microbiol. 2004;70(4):2437–2444.
Edgar RC. MUSCLE: multiple sequence alignment with high accuracy and high throughput. Nucleic Acids Res. 2004;32(5):1792–1797.
Freitag M, Williams RL, Kothe GO, Selker EU. A cytosine methyltransferase homologue is essential for repeat-induced point mutation in *Neurospora crassa*. Proc Natl Acad Sci USA. 2002;99(13):8802–8807.
Gardiner DM, Rusu A, Barrett L, Hunter GC, Kazan K. Can natural gene drives be part of future fungal pathogen control strategies in plants? New Phytol. 2020;228(4):1431–1439.
Geiser DM, Al-Hatmi A, Aoki T, Arie T, Balmas V, Barnes I, Bergstrom GC, Bhattacharyya MKK, Blomquist CL, Bowden R, *et al.* Phylogenomic analysis of a 55.1 kb 19-gene dataset resolves a monophyletic Fusarium that includes the *Fusarium solani* Species Complex. Phytopathology. 2021;111(7):1064–1079.
Gladyshev E. Repeat-induced point mutation and other genome defense mechanisms in fungi. Microbiol. Spectr. 2017;5(4).
Grognet P, Lalucque H, Malagnac F, Silar P. Genes that bias Mendelian segregation. PLoS Genet. 2014;10(5):e1004387.
Hammond TM. Sixteen years of meiotic silencing by unpaired DNA. Adv Genet. 2017;97:1–42.
Hammond TM, Rehard DG, Xiao H, Shiu PK. Molecular dissection of *Neurospora* Spore killer meiotic drive elements. Proc Natl Acad Sci USA. 2012;109(30):12093–12098.
Hammond TM, Xiao H, Rehard DG, Boone EC, Perdue TD, Pukkila PJ, Shiu PK. Fluorescent and bimolecular-fluorescent protein tagging of genes at their native loci in *Neurospora crassa* using specialized double-joint PCR plasmids. Fungal Genet Biol. 2011;48(9):866–873.
Harvey AM, Rehard DG, Groskreutz KM, Kuntz DR, Sharp KJ, Shiu PK, Hammond TM. A critical component of meiotic drive in *Neurospora* is located near a chromosome rearrangement. Genetics. 2014;197(4):1165–1174.
Henderson ST, Eariss GA, Catcheside DEA. Reliable PCR amplification from *Neurospora crassa* genomic DNA obtained from conidia. Fungal Genet. Newsl. 2005;52:24.
Kathariou S, Spieth PT. Spore killer polymorphism in *Fusarium moniliforme*. Genetics. 1982;102(1):19–24.
Kim DE, Chivian D, Baker D. Protein structure prediction and analysis using the Robetta server. Nucleic Acids Res. 2004;32:W526–W531.
Kim H-S, Lohmar JM, Busman M, Brown DW, Naumann TA, Divon HH, Lysøe E, Uhlig S, Proctor RH. Identification and distribution of gene clusters required for synthesis of sphingolipid metabolism inhibitors in diverse species of the filamentous fungus *Fusarium*. BMC Genomics. 2020;21(1):510.
Klittich C, Leslie JF. Nitrate reduction mutants of *Fusarium moniliforme* (*Gibberella fujikuroi*). Genetics. 1988;118(3):417–423.
Kumar S, Stecher G, Li M, Knyaz C, Tamura K. MEGA X: molecular evolutionary genetics analysis across computing platforms. Mol Biol Evol. 2018;35(6):1547–1549.
Leinonen R, H, Sugawara, M, Shumway, C,; International Nucleotide Sequence Database. The sequence read archive. Nucleic Acids Res. 2011;39:D19–D21.
Leslie JF, Dickman MB. Fate of DNA encoding hygromycin resistance after meiosis in transformed strains of *Gibberella fujikuroi* (*Fusarium moniliforme*). Appl Environ Microbiol. 1991;57(5):1423–1429.
Leslie JF, Plattner RD, Desjardins AE, Klittich CJR. Fumonisin B_1 production by strains from different mating populations of *Gibberella fujikuroi* (*Fusarium* section *Liseola*). Phytopathology. 1992;82(3):341–345.
Leslie JF, Summerell BA. The Fusarium Laboratory Manual. Ames, Iowa: Blackwell Publishing; 2006.
Liang J, Fu X, Hao C, Bian Z, Liu H, Xu JR, Wang G. FgBUD14 is important for ascosporogenesis and involves both stage-specific alternative splicing and RNA editing during sexual reproduction. Environ Microbiol. 2021;23(9):5052–5068.
Liu H, Wang Q, He Y, Chen L, Hao C, Jiang C, Li Y, Dai Y, Kang Z, Xu JR. Genome-wide A-to-I RNA editing in fungi independent of ADAR enzymes. Genome Res. 2016;26(4):499–509.
Marasas WF. Discovery and occurrence of the fumonisins: a historical perspective. Environ Health Perspect. 2001;109:239–243.
McCluskey K, Wiest A, Plamann M. The fungal genetics stock center: a repository for 50 years of fungal genetics research. J Biosci. 2010;35(1):119–126.
Milne I, Bayer M, Cardle L, Shaw P, Stephen G, Wright F, Marshall D. Tablet-next generation sequence assembly visualization. Bioinformatics. 2010;26(3):401–402.
Munkvold GP, Proctor RH, Moretti A. Mycotoxin production in *Fusarium* according to contemporary species concepts. Annu Rev Phytopathol. 2021;59:373–402.
Ninomiya Y, Suzuki K, Ishii C, Inoue H. Highly efficient gene replacements in *Neurospora* strains deficient for nonhomologous end-joining. Proc Natl Acad Sci USA. 2004;101(33):12248–12253.
O'Donnell K, Cigelnik E, Nirenberg HI. Molecular systematics and phylogeography of the *Gibberella fujijuroi* species complex. Mycologia. 1998;90(3):465–493.
Pelechano V, Steinmetz LM. Gene regulation by antisense transcription. Nat Rev Genet. 2013;14(12):880–893.
Perkins DD. Wild type *Neurospora crassa* strains preferred for use as standards. Fungal Genet. Newsl. 2004;51(1):7–8.
Perkins DD, ARadford A, Sachs MS. The *Neurospora* compendium: chromosomal loci. San Diego, CA: Academic Press; 2000.
Proctor RH, Desjardins AE, Plattner RD, Hohn TM. A polyketide synthase gene required for biosynthesis of fumonisin mycotoxins in *Gibberella fujikuroi* mating population A. Fungal Genet Biol. 1999;27(1):100–112.
Proctor RH, Van Hove F, Susca A, Stea G, Busman M, van der Lee T, Waalwijk C, Moretti A, Ward TJ. Birth, death and horizontal transfer of the fumonisin biosynthetic gene cluster during the evolutionary diversification of *Fusarium*. Mol Microbiol. 2013;90(2):290–306.
Pyle J, Patel T, Merrill B, Nsokoshi C, McCall M, Proctor RH, Brown DW, Hammond TM. A meiotic drive element in the maize pathogen *Fusarium verticillioides* is located within a 102 kb region of chromosome V. G3 (Bethesda). 2016;6(8):2543–2552.

Raju NB. Ascomycete spore killers: chromosomal elements that distort genetic ratios among the products of meiosis. Mycologia. 1994;86(4):461–473.

Rhoades NA, Harvey AM, Samarajeewa DA, Svedberg J, Yusifov A, Abusharekh A, Manitchotpisit P, Brown DW, Sharp KJ, Rehard DG, *et al.* Identification of *rfk-1*, a meiotic driver undergoing RNA editing in *Neurospora*. Genetics. 2019;212(1):93–110.

Rhoades NA, Webber EK, Hammond TM. A nonhomologous end-joining mutant for *Neurospora sitophila* research. Fungal Genet. Rep. 2020;64. https://doi.org/10.4148/ 1941-4765.2172

Salch YP, Beremand MN. *Gibberella pulicaris* transformants: state of transforming DNA during asexual and sexual growth. Curr Genet. 1993;23(4):343–350.

Samarajeewa DA, Sauls PA, Sharp KJ, Smith ZJ, Xiao H, Groskreutz KM, Malone TL, Boone EC, Edwards KA, Shiu PKT, *et al.* Efficient detection of unpaired DNA requires a member of the Rad54-like family of homologous recombination proteins. Genetics. 2014; 198(3):895–904.

Saupe SJ. The [Het-s] prion of *Podospora anserina* and its role in heterokaryon incompatibility. Semin Cell Dev Biol. 2011;22(5):460–468.

Scauflaire J, Gourgue M, Munaut F. *Fusarium temperatum* sp. nov. from maize, an emergent species closely related to *Fusarium subglutinans*. Mycologia. 2011;103(3):586–597.

Shiu PK, Zickler D, Raju NB, Ruprich-Robert G, Metzenberg RL. SAD-2 is required for meiotic silencing by unpaired DNA and perinuclear localization of SAD-1 RNA-directed RNA polymerase. Proc Natl Acad Sci USA. 2006;103(7):2243–2248.

Sidhu GS. Genetics of *Gibberella fujikuroi* V. Spore killer alleles in *G. fujikuroi*. J Heredity. 1984;75(3):237–238.

Sikhakolli UR, Lopez-Giraldez F, Li N, Common R, Townsend JP, Trail F. Transcriptome analyses during fruiting body formation in *Fusarium graminearum* and *Fusarium verticillioides* reflect species life history and ecology. Fungal Genet Biol. 2012;49(8):663–673.

Steenwyk JL, Shen XX, Lind AL, Goldman GH, Rokas A. A robust phylogenomic time tree for biotechnologically and medically important fungi in the genera *Aspergillus* and *Penicillium*. mBio. 2019; 10(4):1–25.

Svedberg J, Hosseini S, Chen J, Vogan AA, Mozgova I, Hennig L, Manitchotpisit P, Abusharekh A, Hammond TM, Lascoux M, *et al.* Convergent evolution of complex genomic rearrangements in two fungal meiotic drive elements. Nat Commun. 2018;9(1):4242.

Svedberg J, Vogan AA, Rhoades NA, Sarmarajeewa D, Jacobson DJ, Lascoux M, Hammond TM, Johannesson H. An introgressed gene causes meiotic drive in *Neurospora sitophila*. Proc Natl Acad Sci USA. 2021;118(17):e2026605118.

Szewczyk E, Nayak T, Oakley CE, Edgerton H, Xiong Y, Taheri-Talesh N, Osmani SA, Oakley BR, Oakley B. Fusion PCR and gene targeting in *Aspergillus nidulans*. Nat Protoc. 2006;1(6):3111–3120.

Tuite J. Plant Pathological Methods: Fungi and Bacteria. Minneapolis (MN): Burgess Publishing Company; 1969.

Turgeon BG, Garber RC, Yoder OC. Development of a fungal transformation system based on selection of sequences with promoter activity. Mol Cell Biol. 1987;7(9):3297–3305.

Turner BC, Perkins DD. Spore killer, a chromosomal factor in *Neurospora* that kills meiotic products not containing it. Genetics. 1979;93(3):587–606.

Vogan AA, Ament-Velásquez SL, Granger-Farbos A, Svedberg J, Bastiaans E, Debets AJ, Coustou V, Yvanne H, Clavé C, Saupe SJ, *et al.* Combinations of *Spok* genes create multiple meiotic drivers in *Podospora*. eLife. 2019;8:e46454.

Vogel HJ. A convenient growth medium for *Neurospora* (Medium N). Microbial. Genet Bull. 1956;13:42–43.

Wedell N, Price TAR, Lindholm AK. Gene drive: progress and prospects. Proc Biol Sci. 2019;286(1917):20192709.

White DG. Compedium of Corn Diseases. St. Paul (MN): APS Press; 1999.

Xu JR, Leslie JF. A genetic map of *Gibberella fujikuroi* mating population A (*Fusarium moniliforme*). Genetics. 1996;143(1):175–189.

Xue KS, Tang L, Sun G, Wang S, Hu X, Wang JS. Mycotoxin exposure is associated with increased risk of esophageal squamous cell carcinoma in Huaian area, China. BMC Cancer. 2019;19(1):1218.

Zimmering S, Sandler L, Nicoletti B. Mechanisms of meiotic drive. Annu Rev Genet. 1970;4:409–436.

Communicating editor: M. Freitag